NASA CR-145126

Transmission of Sound Through Nonuniform Circular Ducts with Compressible Mean Flows

By
A. H. Nayfeh
B. S. Shaker
J. E. Kaiser

Prepared under Contract No. NAS1 - 13884
By
Virginia Polytechnic Institute and State University
Blacksburg, Virginia
for

NASA
National Aeronautics and
Space Administration

TRANSMISSION OF SOUND THROUGH NONUNIFORM CIRCULAR DUCTS WITH COMPRESSIBLE MEAN FLOWS

by

A. H. Nayfeh

B. S. Shaker

J. E. Kaiser

Department of Engineering Science and Mechanics
Virginia Polytechnic Institute and State University
Blacksburg, Virginia

May 1977

Page
Intentionally
Left Blank

1. Report No.	2. Government Accession No.	3. Recipient's Catalog No.
NASA CR-145126		

4. Title and Subtitle	5. Report Date
TRANSMISSION OF SOUND THROUGH NONUNIFORM CIRCULAR DUCTS WITH COMPRESSIBLE MEAN FLOWS	May 1977
	6. Performing Organization Code
7. Author(s)	8. Performing Organization Report No.
A. H. NAYFEH, B. S. SHAKER, J. E. KAISER	VPI E-77-2
	10. Work Unit No.
9. Performing Organization Name and Address	
Virginia Polytechnic Institute & State University Department of Engineering Science & Mechanics Blacksburg, Virginia 24061	11. Contract or Grant No. NAS1-13884
	13. Type of Report and Period Covered
12. Sponsoring Agency Name and Address	Contractor Report
National Aeronautics and Space Administration Washington, D.C. 20546	14. Sponsoring Agency Code

15. Supplementary Notes

Report on Phase I of work performed for Langley Research Center

16. Abstract

An acoustic theory is developed to determine the sound transmission and attenuation through an infinite, hard-walled or lined, circular duct carrying compressible, sheared, mean flows and having a variable cross section. The theory is applicable to large as well as small axial variations, as long as the mean flow does not separate. Although the theory is described for circular ducts, it is applicable to other duct configurations - annular, two-dimensional, and rectangular. The theory is described for the linear problem, but the technique is general and has the advantage of being applicable to the nonlinear case as well as the linear case.

The technique is based on solving for the envelopes of the quasi-parallel acoustic modes that exist in the duct instead of solving for the actual wave, thereby reducing the computational time and the round-off error encountered in purely numerical techniques. A computer program has been developed based on this theory. The mean-flow model consists of a one-dimensional flow in the core and a quarter-sine profile in the boundary layer. Results are presented for the reflection and transmission coefficients in ducts with varying slopes and carrying different mean flows.

17. Key Words (Suggested by Author(s))	18. Distribution Statement
Duct acoustics Noise control	Unclassified – Unlimited STAR Category 23

19. Security Classif. (of this report)	20. Security Classif. (of this page)	21. No. of Pages	22. Price*
Unclassified	Unclassified	62	

*For sale by the National Technical Information Service, Springfield, Virginia 22151

Page
Intentionally
Left Blank

Table of Contents

1. INTRODUCTION

The present practice of using high-bypass turbojet engines has resulted in a decrease in jet noise. However, these engines emit noise from their inlet nacelles above a desirable level. The present work is part of a considerable effort being made to reduce nacelle noise.

One promising approach to the reduction of inlet noise is the use of a high subsonic Mach number inlet, or partially choked inlet, in conjunction with an acoustic duct liner. The use of choked inlets has long been recognized as an effective means of reducing upstream propagation although such inlets require careful design to prevent excessive losses in compressor performance. However, the physical mechanisms responsible for the noise reduction in high-subsonic Mach number inlets are not completely understood, and techniques for the theoretical analysis of sound propagation through regions of near-sonic mean flow are not available. Two major problems must be overcome in the development of such a model: (1) the mathematical techniques for the calculation of sound propagation in ducts are well-developed for parallel ducts but are not fully developed for ducts of varying cross section that carry mean flows with strong axial and transverse gradients; (2) linear acoustic equations are inadequate to describe acoustic propagation in regions of near-sonic mean flows. In the investigation presented here, the first of these two problems was addressed, and a wave-envelope technique based on the method of variation of parameters was developed. This procedure can be used as the basis of the examination of the second aspect of the problem,

the development of nonlinear models for the near-sonic region.

The concept of sound reduction by choked inlets has been investigated experimentally at great length. The first contribution to the sonic inlet concept goes back to 1960 when Maestrello[1] used a translating centerbody that could be adjusted to vary the inlet throat area. His experiment showed a 35 dB noise reduction at an inlet throat Mach number of 0.9.

Several experimental investigators followed Maestrello to test actual jet engines with various shapes of centerbodies as well as experimental ducts to choke the flow. Surveys of the concept of the choked inlet were given by Lumsdaine[2] and Klujber[3]. An updated survey is presented here.

Sobell and Welliver[4] tested a Bristol Olympus 6 jet engine; this engine was choked by using a sonic block silencer. The background noise radiation associated with this experiment may be a reason why only a 12 dB noise reduction was achieved. Greatrex[5] conducted an experiment on an Avon engine with a bullet shaped centerbody to choke the flow. He reported a 20 dB noise reduction.

To test the effect of choking the flow on the reduction of inlet noise, Sawhill[6] tested an ST model inlet with a translating centerbody and reported a 33 dB noise reduction when the throat Mach number of the inlet was increased from 0.63 to 0.9. Cawthorn et al[7] tested an SST inlet with a Viper 8 turbojet engine and a translating centerbody to choke the flow. They found that choking the flow resulted only in a 3 dB noise reduction. Using two centerbodies of different

sizes to choke the flow of an SST inlet, Anderson[8] obtained a 20 dB noise reduction at a throat Mach number of 0.77.

Schaut[9] tested a T-50 engine to show the acoustic and internal flow characteristics of airfoil grid inlets. The configuration consisted of an inlet duct with two rows of two-dimensional airfoils; the flow Mach number between the airfoils was maintained at a transonic level to reduce noise radiation from the inlet. A 13 dB noise reduction was measured at a Mach number of 0.9. Another test was conducted by Anderson et al[10] on the airfoil grid inlet; they used two airfoils positioned in parallel in an inlet duct. They reported a loss of 7% in the inlet recovery pressure when they attained a 27 PNdB noise reduction.

Inlet guide vanes also have a significant effect on the noise reduction. Chestnutt and Stewart[11] conducted an experiment by using an accelerating inlet. They reported noise reductions up to 25 dB, due to the elimination of multiple pure tones, when the inlet approached choking conditions. The only drawback is that the noise reduction was accompanied by a significant reduction in the compressor efficiency. To determine the effect of the shape of the guide vane on the noise reduction, Chestnutt[12] tested uncambered and tapered inlet guide vanes. He obtained noise reductions of about 28 dB and 36 dB for the uncambered and tapered guide vanes, respectively. Anderson et al[10] tested radial vane inlets and showed a 22.5 PNdB noise reduction with a 7% loss in recovery pressure.

Copeland[13] studied the noise radiation from a rotor in a lined annular duct at high subsonic Mach number. He achieved about 7 dB reduction in the overall noise when he increased the duct length by a factor of 4.

Hawking and Lawson[14] reported a large reduction in acoustic energy for a waisted geometry. They suggested that this reduction is due to an increase in the axial Mach number. Benzakin et al[15] conducted an experiment on a lined accelerating inlet. They concluded that the noise increases with increasing Mach number until throat Mach numbers of 0.6, then the noise level goes down with further increases in throat Mach number.

It is clear from the above experiments that inlet choking may be an effective noise suppression mechanism. The amount of noise reduction depends on how the choking is achieved. However, the choking may be accompanied by a loss in the compressor efficiency. Thus, the optimum choking configuration is the one accompanied by no loss or a minor loss in the compressor efficiency.

Many investigators studied the possibility of attaining a significant noise reduction with a minor loss in the compressor efficiency; they showed that the loss in the compressor efficiency can be minimized by carefully designing the centerbody.

Klujber[16] reported a noise reduction when a sonic inlet is used. This reduction occurs when the average throat Mach number increases from 0.5 to 1.0. He reported also that more reduction of the noise can be attained but with a further decrease in the inlet recovery pressure.

Higgins et al[17] measured a significant noise reduction with a moderate loss in recovery pressure by using variable cowl inlets. Lumsdaine et al[18] studied experimentally inlets with translating centerbodies; they showed that translating centerbody inlets are superior aerodynamically and more effective in reducing the noise than

collapsing cowl inlets. Koch et al[19] reported a 15 dB sound level attenuation with a minimum loss of aerodynamic performance when operating at an average Mach number of 0.79. Miller and Abbott[20] tested experimentally an inlet with a translating centerbody to choke the flow; they reported a 20 dB noise reduction with a pressure recovery of 98.5%. Abbott[21] indicated that the most efficient method to achieve aerodynamic performance and noise reduction is to use a cylindrical centerbody at takeoff and a bulb-shaped centerbody at approach to choke the flow. He reported that increasing the inlet length results in a higher recovery pressure for a given noise reduction. Groth[22] tested a J-85 turbojet engine using a translating centerbody inlet with a radial vane. He measured a 40 dB reduction in a fully choked inlet while maintaining a recovery pressure of 92.1%. Savkar and Kazin[23] showed that a 99% recovery pressure can be attained for the same amount of noise reduction by proper contouring of the centerbody and careful designing of the diffuser. Miller[24] experimentally determined how a sonic inlet can be designed to have a significant noise reduction with a minimum loss of total pressure.

As we see above, most, but not all, of these investigations have noted significant reductions of the noise level when the inlet is choked. The geometry of the inlet, the geometry of the centerbody and the operating condition seem to have an effect on the acoustic as well as on the aerodynamic performance. Further, most of the potential noise reduction is achieved by operation in the partially choked state (mean Mach number in the throat of 0.8-0.9). Some investigators (e.g., Chestnutt and Clark[25] and Sobel and Welliver[4]) report the possibility

of substantial "leakage" through the wall boundary layers, whereas others (e.g. Klujber[16]) report that such leakage is minor. Although the experimental studies have demonstrated that the choked inlet is a viable technique, they have not provided insight into the physical mechanisms that are responsible for the noise reduction or that explain the differences among the several experimental resutls.

Several analytical as well as numerical techniques have been developed for the analysis of wave propagation in uniform and nonuniform ducts. Surveys of these techniques were made by Nayfeh et al[26] and Nayfeh[27]. In this study, only a short critique is presented.

The problem of sound propagation in a uniform duct (rectangular, circular, etc.), with or without mean flows, for hard as well as lined walled ducts, has been studied extensively. A number of parametric studies have been done for the case of uniform ducts, showing the effect of each parameter on noise attenuation. A large number of papers are cited in the review article of Nayfeh et al[26], each of which discusses at least one of the acoustic parameters.

The investigation of the problem of sound propagation in nonuniform ducts was motivated by the experimental discoveries discussed earlier in this introduction. These investigations are discussed below in order of increasing complexity of the mean flow: no flow; one-dimensional flow; and two-dimensional flow.

The problem of sound propagation in a variable-area duct with no-mean flow was discussed for horns by Webster[28]. He considered only the lowest propagating mode. Stevenson[29] extended Webster's work to investigate the propagation of various modes. He used the method of weighted

residuals to solve the problem of wave propagation in hard-walled horns of arbitrary shape. Eversman et al[30] extended the method of weighted residuals to study multimodal propagation in a nonuniform lined duct.

Alfredson[31] divided the variable area duct into a finite number of stepped uniform ducts. Thus, a large number of stepped uniform ducts are needed to provide sufficient accuracy for cases with large axial gradients.

Nayfeh and Telionis[32] used the method of multiple scales to analyze wave propagation in ducts with slowly, but arbitrarily, varying cross sections and wall admittance. For the case of hard-walled ducts, the solution of Nayfeh and Telionis is equivalent to that of Stevenson for slowly varying ducts. Nayfeh and Telionis pointed out that both of the solutions break down near cut-off; they suggested using a turning point analysis (see 7.3.2 of Reference 33) to overcome this problem.

Isakovitch[34], Samuels[35] and Salant[36] obtained perturbation solutions for wave propagation in ducts whose rigid walls have sinusoidal undulations of small amplitudes. Their perturbation expansions are not valid near resonance conditions; that is, whenever the wave number of the wall undulation is approximately equal to the sum or difference of the wave numbers of any two acoustic modes. Nayfeh[37] used the method of multiple scales to obtain an expansion valid near resonance. He found that neither of the modes involved in the resonance can propagate in the duct without exciting the other.

Quinn[38] and Baumeister and Rice[39] developed finite difference methods to study a plane wave propagating in nonuniform ducts. We note that a large amount of computation will be required with these

purely numerical techniques because a large number of grid points are needed to provide sufficient accuracy. The axial step must be small enough to resolve the smallest wave length, while the transverse step must be small enough to resolve the highest mode. Thus, the computational time increases rapidly with increasing frequency and duct length. To reduce the computational time for plane waves in a two-dimensional duct, Baumeister[40] expressed the potential function $\phi(x,y,t)$ as $\psi(x,y)$ $\exp[i(kx - \omega t)]$, where k is a properly chosen constant, such as the wavenumber in a hard-walled duct. Then he solved for $\psi(x,y)$ using finite differences.

Approximating the mean flow by a quasi-one-dimensional flow, Powell[41] used a multiple reflection method to study the acoustic propagation through variable-area ducts. Eisenberg and Kao[42] analyzed plane waves in a variable area duct that yields an equation with constant coefficients. Davis and Johnson[43] used a forward-integration technique to solve the acoustic equation describing the axial variations. Huerre and Karamcheti[44] analyzed the propagation of the lowest mode by using the WKB approximation, while King and Karamcheti[45] developed a second-order-accurate numerical method to solve for the propagation through a variable area duct by using the method of characteristics.

Nayfeh and co-workers studied extensively the propagation of various acoustic modes in ducts having slowly varying cross sections and carrying general mean flows. Nayfeh et al[46] discussed the acoustic propagation in lined plane ducts with varying cross sections and sheared mean flow. This work was extended to annular ducts by Nayfeh et al[47]. The effect of a compressible sheared mean flow on sound transmission through a

variable-area plane duct was studied by Nayfeh and Kaiser[48]. Using their method, one can determine the transmission and attenuation of all modes including the effect of transverse as well as axial gradients, but the technique is limited to slow variations. Moreover, the expansion needs to be carried out to second order in order to determine reflection of the acoustic signal.

Eversman[49] developed a theory by using the method of weighted residuals to determine the transmission of sound in plane nonuniform hard-walled ducts with mean flow. He obtained equations describing the axial variations of the modes. To solve these equations, one needs a large number of axial steps, especially as the mean Mach number approaches unity and the frequency becomes large, leading to a rapid decrease in the axial wavelength.

In summary, purely numerical techniques suffer from the requirement of large computation times, and they have been restricted thus far to cases of no-mean flow. Analytical techniques have only been applied thus far to simple cases of one-dimensional mean flows and/or plane acoustic waves and/or slowly varying duct geometry and promise to become unwieldy for more general cases. Thus, the specific analytical and computational tools that are needed for the study of wave propagation in ducts involving large gradients in both the axial and transverse directions are lacking.

In this study an acoustic theory is developed to determine the sound transmission and attenuation through an infinite, hard-walled or lined circular duct carrying compressible, sheared, mean flows and having a variable cross section. The theory is applicable to large

as well as small axial variations, as long as the mean flow does not separate. The technique is based on solving for the envelopes of the quasi-parallel acoustic modes that exist in the duct instead of solving for the actual wave. The feasibility of this technique has been demonstrated by Kaiser and Nayfeh[50] for plane ducts with no-mean flow.

The problem is formulated in the following section, the method of solution is presented in Section 3, the numerical solution is described in Section 4, the numerical results and discussion are presented in Section 5, and the conclusions and recommendations are presented in Section 6.

2. PROBLEM FORMULATION

The transmission and attenuation of sound in hard- and soft-walled circular inlet ducts (Figure 1) carrying viscous or inviscid high subsonic mean flows is examined. The mean Mach number in the throat is near sonic; thus, the axial and radial gradients of the mean flow are large. The cross section of the duct varies arbitrarily with the axial distance.

It is convenient to work with dimensionless quantities. To this end, velocities, lengths, and time are made dimensionless by using the ambient speed of sound c_a, the radius R_0 of the duct in the uniform region (Figure 1) and R_0/c_a, respectively. The pressure p is made dimensionless by using $\rho_a c_a^2$, the density ρ and temperature T are made dimensionless by using their corresponding ambient values, while the viscosity μ and the thermal conductivity κ are made dimensionless by using their corresponding wall values in the uniform section. In terms of these dimensionless variables, the equations which describe the unsteady viscous flow in a duct are (see for example, Schlichting[51]).

conservation of mass

$$\frac{\partial \rho}{\partial t} + \nabla \cdot (\rho \vec{v}) = 0 \tag{1}$$

conservation of momentum

$$\rho\left(\frac{\partial \vec{v}}{\partial t} + \vec{v} \cdot \nabla \vec{v}\right) = - \nabla p + \frac{1}{Re} \nabla \cdot \underline{\underline{\tau}} \tag{2}$$

conservation of energy

$$\rho\left(\frac{\partial T}{\partial t} + \vec{v} \cdot \nabla T\right) - (\gamma-1)\left(\frac{\partial p}{\partial t} + \vec{v} \cdot \nabla p\right) =$$

$$\frac{1}{Re}\left[\frac{1}{Pr} \nabla \cdot (\kappa \nabla T) + (\gamma-1)\Phi\right] \tag{3}$$

equation of state

For a perfect gas,

$$\gamma p = \rho T \tag{4}$$

where $\vec{v}$ is the velocity vector, t is the time, γ is the ratio of the gas specific heats, $Pr = \mu_w C_p/\kappa_w$ is the Prandtl number, C_p is the gas specific heat at constant pressure, and $Re = \rho_a c_a R_0/\mu_w$ is the Reynolds number. For a Newtonian fluid, the dimensionless viscous-stress tensor $\underline{\underline{\tau}}$ and the dimensionless dissipation function Φ are related to $\vec{v}$ by

$$\underline{\underline{\tau}} = \mu[\nabla\vec{v} + (\nabla\vec{v})^*] + \lambda \nabla \cdot \vec{v}$$

$$\Phi = \underline{\underline{\tau}} : \nabla\vec{v} = \sum_{j=1}^{3} \sum_{i=1}^{3} \tau_{ij} \partial v_i/\partial x_j$$

where $(\nabla\vec{v})^*$ denotes the transpose of $\nabla\vec{v}$.

In general, the ducts carry a high subsonic, steady, sheared mean flow that satisfies equations (1) through (4). The presence of sound in the ducts results in the perturbation of the flow quantities so that

$$q(\vec{r},t) = q_0(\vec{r}) + q_1(\vec{r},t) \tag{5}$$

where q stands for any flow quantity, $\vec{r}$ is the position vector, q_0 is

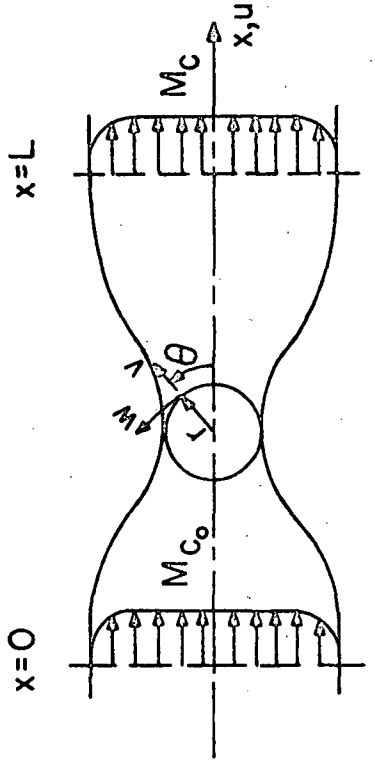

Figure 1. Duct configuration and coordinate system.

the mean-flow part, and q_1 is the acoustic part. Substituting equation (5) into equations (1) through (4) and eliminating the mean-flow quantities, one obtains the following acoustic equations:

$$\frac{\partial \rho_1}{\partial t} + \nabla \cdot (\rho_0 \vec{v}_1 + \rho_1 \vec{v}_0) = NL \tag{6}$$

$$\rho_0 \left(\frac{\partial \vec{v}_1}{\partial t} + \vec{v}_0 \cdot \nabla \vec{v}_1 + \vec{v}_1 \cdot \nabla \vec{v}_0\right) + \rho_1 \vec{v}_0 \cdot \nabla \vec{v}_0 =$$

$$- \nabla p_1 + \frac{1}{Re} \nabla \cdot \underline{\underline{\tau}}_1 + NL \tag{7}$$

$$\rho_0 \left(\frac{\partial T_1}{\partial t} + \vec{v}_0 \cdot \nabla T_1 + \vec{v}_1 \cdot \nabla T_0\right) + \rho_1 \vec{v}_0 \cdot \nabla T_0 - (\gamma - 1)\left(\frac{\partial p_1}{\partial t}\right.$$

$$\left. + \vec{v}_0 \cdot \nabla p_1 + \vec{v}_1 \cdot \nabla p_0\right) = \frac{1}{Re} \left[\frac{1}{Pr} \nabla \cdot (\kappa_0 \nabla T_1 + \kappa_1 \nabla T_0)\right.$$

$$\left. + (\gamma - 1)\Phi_1\right] + NL \tag{8}$$

$$\frac{p_1}{p_0} = \frac{\rho_1}{\rho_0} + \frac{T_1}{T_0} \tag{9}$$

where $\underline{\underline{\tau}}$ and Φ_1 are linear in the acoustic quantities and NL stands for the nonlinear terms in the acoustic quantities.

No solution to equations (6) through (9) subject to general initial and boundary conditions is available yet. To determine solutions for the propagation of sound in ducts, researchers have used simplifying assumptions. Here, the nonlinear and viscous terms in the acoustic equations are neglected, and the mean flow is taken to be a function of the axial and radial coordinates only. Thus, we neglect swirling mean flows. The assumption of linearization is not valid for high sound-pressure levels. The effects of the nonlinear acoustic properties of the lining material become significant when the sound-

pressure level exceeds about 130 dB (re 0.0002 dyne/cm) while the effects of the gas nonlinearity become significant when the sound pressure level exceeds about 160 dB. In particular, the nonlinearity of the gas must be included when the mean flow is transonic (i.e., near the throat). Nayfeh[52] showed that the viscous terms in the acoustic equations produce an effective admittance at the wall that leads to small dispersion and attenuation. For lined ducts, this admittance produced by the acoustic boundary layer may be neglected, but it cannot be neglected for hard-walled ducts as demonstrated analytically and experimentally by Pestorius and Blackstock[53].

A cylindrical coordinate system (r,θ,x) is introduced as shown in Figure 1. Since there is no swirling flow, each flow quantity $q_1(r,x,\theta,t)$ can be expressed, for sinusoidal time variations, as

$$q_1(r,x,\theta,t) = \sum_{m=0}^{\infty} q_{1m}(r,x)\exp[-i(\omega t + m\theta)] \tag{10}$$

where ω is the dimensionless frequency. Using the above assumptions, one can rewrite equations (6) through (9) in cylindrical coordinates as

$$-i\omega\rho_1 + \frac{\partial}{\partial x}(\rho_0 u_1 + u_0\rho_1) + \frac{i\rho_0 m}{r} w_1 + \frac{1}{r}\frac{\partial}{\partial r}(r\rho_0 v_1 + rv_0\rho_1) = 0 \tag{11}$$

$$\rho_0\left[-i\omega u_1 + \frac{\partial}{\partial x}(u_0 u_1) + v_0\frac{\partial u_1}{\partial r} + v_1\frac{\partial u_0}{\partial r}\right] + \rho_1\left[u_0\frac{\partial u_0}{\partial x} + v_0\frac{\partial u_0}{\partial r}\right] = -\frac{\partial p_1}{\partial x} \tag{12}$$

$$\rho_0\left[-i\omega v_1 + \frac{\partial}{\partial r}(v_0 v_1) + u_0\frac{\partial v_1}{\partial x} + u_1\frac{\partial v_0}{\partial x}\right] + \rho_1\left[v_0\frac{\partial v_0}{\partial r} + u_0\frac{\partial v_0}{\partial x}\right] = -\frac{\partial p_1}{\partial r} \tag{13}$$

$$\rho_0\left[-i\omega w_1 + v_0 \frac{\partial w_1}{\partial r} + \frac{v_0 w_1}{r} + u_0 \frac{\partial w_1}{\partial x}\right] = -\frac{im}{r} p_1 \tag{14}$$

$$\rho_0\left[-i\omega T_1 + v_0 \frac{\partial T_1}{\partial r} + u_0 \frac{\partial T_1}{\partial x} + v_1 \frac{\partial T_0}{\partial r} + u_1 \frac{\partial T_0}{\partial x}\right] + \rho_1\left[v_0 \frac{\partial T_0}{\partial r} + u_0 \frac{\partial T_0}{\partial x}\right] - (\gamma-1)\left[-i\omega p_1 + u_0 \frac{\partial p_1}{\partial x} + v_0 \frac{\partial p_1}{\partial r} + u_1 \frac{\partial p_0}{\partial x} + v_1 \frac{\partial p_0}{\partial r}\right] = 0 \tag{15}$$

$$\frac{p_1}{p_0} = \frac{\rho_1}{\rho_0} + \frac{T_1}{T_0} \tag{16}$$

where u, v, and w are the velocities in the axial, radial, and azimuthal directions, respectively, and the subscript m has been suppressed.

To complete the problem formulation, one needs to specify the initial and boundary conditions. The boundary conditions are based on the assumption that the duct wall is lined with a point-reacting acoustic material whose specific acoustic admittance β may vary along the duct. For no-slip mean flow, a requirement of continuity of the particle displacement gives

$$v_1 - R'u_1 = \frac{\beta}{\rho_w c_w} p_1 \sqrt{1 + R'^2} \qquad \text{at } r = R \tag{17}$$

where R' is the slope of the wall and the subscript w refers to values at the wall.

3. METHOD OF SOLUTION

3.1 Critique of the Existing Methods

Since there is no exact solution available yet for equations (11) through (16) in ducts of varying cross sections and since purely numerical solutions of this problem are not feasible owing to the excessive amount of computation time needed, a number of approaches have been developed to determine approximate solutions to this problem[26,27]. These approaches include quasi-one-dimensional approximations, solutions for slowly varying cross sections, solutions for weak wall undulations, variational methods, and approximation of the duct by a series of stepped uniform cross sections. A short critique of these approaches is discussed next (more detailed critiques are given in references 26 and 27), and it is followed by the proposed acoustic-wave-envelope technique.

In the quasi-one-dimensional approach, one can determine only the lowest mode in ducts with slowly varying cross sections and cannot account for transverse mean-flow gradients or large wall admittance.

In the slowly varying cross-section approach, one can determine the transmission and attenuation for all modes including the effects of transverse as well as axial gradients, but the technique is limited to slow variations and the expansion needs to be carried out to second order to determine reflections of the acoustic signal.

In the weak-wall-undulation approach, one assumes that the dimensionless duct radius is described by $R = 1 + \varepsilon R_1(x)$, where ε is small.

Thus, in this approach one can account for all effects except large axial variations.

In the variational approach, one uses either the Rayleigh-Ritz procedure, which requires knowledge of the Lagrangian describing the problem, or the Galerkin procedure (the method of weighted residuals). Since the Lagrangian is not known yet for the general problem, the Galerkin procedure is the only applicable technique at this time. According to this procedure, one chooses basis functions (usually the mode shapes of a quasi-parallel problem) and represents the pressure, for example, as

$$p_1 = \sum_{n=1}^{\infty} p_n(x)\psi_n(r,x) \tag{18}$$

where the ψ_n are the basis functions which, in general, do not satisfy the boundary conditions. On expanding all flow variables in the form of equation (18), substituting the result into equations (11) through (17), and using the Galerkin procedure to minimize the error, one obtains differential equations describing the p_n. Since the ψ_n do not satisfy the equations and the boundary conditions, a large number of terms are needed to satisfy the equations and the boundary conditions and hence represent the solution for large cross sectional variations; this leads to serious convergence questions. These problems can be minimized by choosing the ψ_n to be the quasi-parallel mode shapes corresponding to the propagation constants k_n. The functions $p_n(x)$ vary rapidly even for a uniform duct: $p_n(x) \propto \exp(ik_n x)$, and k_n can be very large for high frequency, low-order modes. Thus, very small

axial steps must be used in the computations, resulting in a large computation time, which increases very rapidly with axial distance and sound frequency.

In approximating a duct with a continuously varying cross-sectional area by a series of stepped uniform ducts, a large number of uniform segments are needed to provide sufficient accuracy for the solution when the axial gradients are large. Thus, this approach is impractical in the present problem because an enormous amount of computation time is needed even for the case of a moderate number of uniform segments.

This short discussion shows that presently available techniques would certainly fail to produce sufficient accuracy for the present problem. Thus, alternate techniques must be developed. In addition, purely numerical techniques would be impractical because of the excessive amount of computation time. This is a result of the necessity of using very small axial and radial steps to represent the rapidly varying mode shapes and the axial oscillations of each mode. (In fact, a computational difficulty exists in calculating the higher-order Bessel functions that represent the mode shapes in a uniform duct carrying uniform mean flow unless asymptotic expansions are used.) Moreover, the axial step must be much smaller than the wavelength of the lowest mode in order to be able to determine the axial variations. These small steps would cause the error in the numerical solution to increase very rapidly with axial distance. Similar problems have been encountered by astronomers who developed what is usually called the special perturbation method in which one solves only for the wave

envelope instead of solving for the wave itself. Here, we use this idea to develop a wave-envelope technique for solving the present problem.

3.2 Form of Solution

According to this approach, one uses the method of variation of parameters to change the dependent variables from the fast-varying variables to others that vary slowly. Moreover, the solution is approximated by a finite sum of the quasi-parallel duct eigenfunctions.

Thus, we seek an approximate solution to equations (11) through (17) in the form

$$p_1 \approx \sum_{n=1}^{N} \left\{ A_n(x)\psi_n^p(r,x)\exp\left(i\int k_n(x)dx\right)+\tilde{A}_n(x)\tilde{\psi}_n^p(r,x)\exp\left(i\int \tilde{k}_n(x)dx\right)\right\} \tag{19}$$

$$u_1 \approx \sum_{n=1}^{N} \left\{ A_n(x)\psi_n^u(r,x)\exp\left(i\int k_n(x)dx\right) + \tilde{A}_n(x)\tilde{\psi}_n^u(r,x)\exp\left(i\int \tilde{k}_n(x)\,dx\right)\right\} \tag{20}$$

with similar expression for v_1, w_1, T_1, and ρ_1, where the tilde refers to upstream propagation, the $\psi_n(r,x)$ are the quasi-parallel mode shapes corresponding to the quasi-parallel propagation constants $k_n(x)$, and the $A_n(x)$ are complex functions whose moduli and arguments represent, in some sense, the amplitudes and the phases of the (m,n) modes. The circumferential mode number m is assumed to be specified and the corresponding subscript on A, ψ and k is not explicitly stated; each variable is expressed as a summation over a finite number of radial modes n, with n = 1 denoting the fundamental radial mode rather than the conventional n = 0. Since k_n is complex, the exponential factor contains an estimate of the attenuation of the (m,n) mode. Thus, the envelope of the (m,n) mode is given by

$$|A_n(x)| \exp[-\int \alpha_n(x)dx]$$

where α_n is the imaginary part of k_n.

Since the ψ_n are the quasi-parallel mode shapes, they are the solutions of the following problem:

$$- i\hat{\omega}\psi^p + ik\rho_o\psi^u + \frac{i\rho_o m}{r}\psi^w + \frac{1}{r}\frac{\partial}{\partial r}(r\rho_o\psi^v) = 0 \tag{21}$$

$$- i\rho_o\hat{\omega}\psi^u + \rho_o\frac{\partial u_o}{\partial r}\psi^v + ik\psi^p = 0 \tag{22}$$

$$- i\rho_o\hat{\omega}\psi^v + \frac{\partial\psi^p}{\partial r} = 0 \tag{23}$$

$$- i\rho_o\hat{\omega}\psi^w + \frac{im}{r}\psi^p = 0 \tag{24}$$

$$- i\rho_o\hat{\omega}\psi^T + \rho_o\frac{\partial T_o}{\partial r}\psi^v + i(\gamma-1)\hat{\omega}\psi^p = 0 \tag{25}$$

$$\frac{\psi^p}{p_o} = \frac{\psi^\rho}{\rho_o} + \frac{\psi^T}{T_o} \tag{26}$$

$$\psi^v - \frac{\beta}{\rho_w c_w}\psi^p = 0 \quad \text{at} \quad r = R \tag{27}$$

where

$$\hat{\omega} = \omega - ku_o \tag{28}$$

Equations (21) - (28) can be combined to yield the following problem[54] for ψ^p:

$$\frac{\partial^2\psi^p}{\partial r^2} + [\frac{1}{r} + \frac{T_o'}{T_o} + \frac{2ku_o'}{\hat{\omega}}]\frac{\partial\psi^p}{\partial r} + [\frac{\hat{\omega}^2}{T_o} - k^2 - \frac{m^2}{r^2}]\psi^p = 0 \tag{29}$$

$$\frac{\partial\psi^p}{\partial r} - i\frac{\omega\beta}{T_w^{\frac{1}{2}}}\psi^p = 0 \text{ at } r = R \tag{30}$$

At each axial location, the solution of equations (29) and (30) yields $\psi_n^p(r;x)$ and its corresponding propagation constant $k_n(x)$. Since the basis functions $\psi_n^p(r;x)$ vary in the axial direction, they must be nor-

malized in some manner to provide significance to the axial variations of the mode amplitudes. The normalization used in this study is the same as that defined by Zorumski[55]:

$$\int_0^R r[\psi_n^p(r;x)]^2 dr = 1$$

Then, equations (21) - (26) are used to express the mode shapes of the other flow variables in terms of ψ_n^p and k_n.

3.3 Constraints

Since the transverse dependence in the assumed solution, equations (19) and (20), is chosen *a priori*, it cannot satisfy equations (11) - (17) exactly. Thus, the assumed solution must be subjected to constraints. Rather than using the usual method of weighted residuals which forces the residuals in each of the basic equations (11) - (16) and the boundary conditon (17) to be orthogonal to some *a priori* chosen functions, one requires the deviations from the quasi-parallel solution to be orthogonal to every solution of the adjoint quasi-parallel problem. This approach assures the recovery of the results of the method of multiple scales[33] when the axial variations are slow[50].

To enforce the contraints, one must define the problem adjoint to the quasi-parallel problem. To this end, one can multiply equations (21) - (26) by the functions ϕ_1, ϕ_2, ϕ_3, ϕ_4, ϕ_5, and ϕ_6, respectively, where the $\phi_n(r,x)$ are solutions of the adjoint problem, add the resulting equations, integrate the result by parts from r = 0 to r = R thereby transferring the r-derivatives from the ψ's to the ϕ's, and obtain

$$\int_0^R \psi^p[-i\hat{\omega}\phi_1 - T_0 p_0 \phi_6]dr + \int_0^R i\rho_0\psi^u[-\hat{\omega}\phi_2 + k\phi_1]dr + \int_0^R \rho_0\psi^v[-i\hat{\omega}\phi_3 + \frac{\partial u_0}{\partial r}\phi_2 - r\frac{\partial}{\partial r}(\frac{\phi_1}{r}) + \frac{\partial T_0}{\partial r}\phi_5]dr + \int_0^R i\rho_0\psi^w[-\hat{\omega}\phi_4 + \frac{m}{r}\phi_1]dr + \int_0^R \psi^p[ik\phi_2 - \frac{\partial \phi_3}{\partial r} + \frac{im}{r}\phi_4 + i(\gamma-1)\hat{\omega}\phi_5 + \rho_0 T_0\phi_6]dr + \int_0^R \rho_0\psi^T[-i\hat{\omega}\phi_5 - p_0\phi_6]dr + [\rho_0\psi^v\phi_1 + \psi^p\phi_3]_0^R = 0 \quad (31)$$

Then, the adjoint equations are obtained by setting each of the brackets in the integrands of equation (31) to zero; that is

$$i\hat{\omega}\phi_1 + p_0 T_0 \phi_6 = 0 \quad (32)$$

$$-\hat{\omega}\phi_2 + k\phi_1 = 0 \quad (33)$$

$$-i\hat{\omega}\phi_3 + \frac{\partial u_0}{\partial r}\phi_2 - r\frac{\partial}{\partial r}(\frac{\phi_1}{r}) + \frac{\partial T_0}{\partial r}\phi_5 = 0 \quad (34)$$

$$-\hat{\omega}\phi_4 + \frac{m}{r}\phi_1 = 0 \quad (35)$$

$$ik\phi_2 - \frac{\partial \phi_3}{\partial r} + \frac{im}{r}\phi_4 + i(\gamma-1)\hat{\omega}\phi_5 + \rho_0 T_0\phi_6 = 0 \quad (36)$$

$$i\hat{\omega}\phi_5 + p_0\phi_6 = 0 \quad (37)$$

Equation (31) is reduced to

$$(\rho_0\psi^v\phi_1 + \psi^p\phi_3)_{r=0} = (\rho_0\psi^v\phi_1 + \psi^p\phi_3)_{r=R} \quad (38)$$

From equations (32) - (35) and (37), one can express each of the ϕ_n as a function of ϕ_1:

$$\phi_2 = \frac{k}{\hat{\omega}} \phi_1 \tag{39}$$

$$\phi_3 = \frac{irT_0}{\hat{\omega}^2} \frac{\partial}{\partial r} \left(\frac{\hat{\omega}\phi_1}{rT_0}\right) \tag{40}$$

$$\phi_4 = \frac{m\phi_1}{r\hat{\omega}} \tag{41}$$

$$\phi_5 = \frac{\phi_1}{T_0} \tag{42}$$

$$\phi_6 = - ip_0T_0\hat{\omega}\phi_1 \tag{43}$$

Using equations (39) - (43) in equation (36), one then obtains the governing equation for ϕ_1:

$$\frac{1}{r} \frac{\partial}{\partial r} \left[\frac{rT_0}{\hat{\omega}^2} \frac{\partial \eta}{\partial r}\right] + \left[1 - \frac{T_0k^2}{\hat{\omega}^2} - \frac{T_0m^2}{r^2\hat{\omega}^2}\right]\eta = 0 \tag{44}$$

where

$$\eta = \frac{\phi_1\hat{\omega}}{rT_0} \tag{45}$$

It can be shown easily that equations (29) and (44) are the same; thus η and ψ^p satisfy the same differential equation. The boundary conditions on η are obtained from equation (38) by substitution for ψ^v from equation (23), for ϕ_3 from equation (40), and for ϕ_1 from equation (45). The result is

$$\frac{irT_0}{\hat{\omega}^2} \left[- \frac{\partial \psi^p}{\partial r} \eta + \psi^p \frac{\partial \eta}{\partial r}\right]_{r=R} = \frac{irT_0}{\hat{\omega}^2} \left[- \frac{\partial \psi^p}{\partial r} \eta + \psi^p \frac{\partial \eta}{\partial r}\right]_{r=0} \tag{46}$$

If one requires that η be bounded at $r = 0$, just as ψ^p is, then the right-hand side vanishes. The use of equation (30) to eliminate $\partial\psi^p/\partial r$ leads to

$$\psi^p\left[\frac{\partial \eta}{\partial r} - \frac{i\omega\beta}{T_w^{\frac{1}{2}}}\eta\right] = 0 \quad \text{at } r = R$$

Since ψ^p is arbitrary at $r = R$,

$$\frac{\partial \eta}{\partial r} - \frac{i\omega\beta}{T_w^{\frac{1}{2}}}\eta = 0 \quad \text{at } r = R \tag{47}$$

Since the boundary condition (47) is the same as the boundary condition (30), $\eta = \psi^p$, without loss of generality, and hence, one does not need to solve the adjoint problem. One needs only to solve the quasi-parallel problem to determine ψ_n^p and then determine ϕ_{1n} from

$$\phi_{1n} = \frac{rT_0\ \psi_n^p}{\hat{\omega}} \tag{48}$$

according to equation (45). The remaining ϕ's are then determined from equations (39) - (43).

Once the adjoint functions are known, the constraint conditions are determined as follows. On multiplying equations (11) - (16) by ϕ_{1n}, ϕ_{2n}, ..., ϕ_{6n}, respectively, adding the resulting equations, integrating the result by parts from $r = 0$ to $r = R$ to transfer the r-derivatives to the ϕ's, and using equations (32) - (37) and (17), one obtains the following constraint:

$$\int_0^R \Big\{ \phi_{1n}[-iu_0k_n\rho_1 - ik_n\rho_0u_1 + \frac{\partial}{\partial x}(\rho_0u_1 + u_0\rho_1)] - rv_0\rho_1 \frac{\partial}{\partial r}(\frac{\phi_{1n}}{r})$$

$$+ \phi_{2n}[-iu_0k_n\rho_0u_1 - ik_np_1 + \rho_0 \frac{\partial(u_0u_1)}{\partial x} + \rho_1(u_0 \frac{\partial u_0}{\partial x} + v_0 \frac{\partial u_0}{\partial r})$$

$$+ \frac{\partial p_1}{\partial x}] - u_1 \frac{\partial}{\partial r}(\rho_0v_0\phi_{2n}) + \phi_{3n}[-iu_0k_n\rho_0v_1 + \rho_0u_0 \frac{\partial v_1}{\partial x}$$

$$+ \rho_0u_1 \frac{\partial v_0}{\partial x} + \rho_1(v_0 \frac{\partial v_0}{\partial r} + u_0 \frac{\partial v_0}{\partial x})] - v_0v_1 \frac{\partial}{\partial r}(\rho_0\phi_{3n})$$

$$+\phi_{4n}[-ik_n\rho_0u_0w_1 + \frac{\rho_0v_0w_1}{r} + \rho_0u_0 \frac{\partial w_1}{\partial x}] - w_1 \frac{\partial}{\partial r}(\rho_0v_0\phi_{4n})$$

$$+ \phi_{5n}[-iu_0k_n\rho_0T_1 + (\gamma-1)iu_0k_np_1 + \rho_0u_0 \frac{\partial T_1}{\partial x} + \rho_0u_1 \frac{\partial T_0}{\partial x}$$

$$+ \rho_1(v_0 \frac{\partial T_0}{\partial r} + u_0 \frac{\partial T_0}{\partial x}) - (\gamma-1)(u_0 \frac{\partial p_1}{\partial x} + u_1 \frac{\partial p_0}{\partial x} + v_1 \frac{\partial p_0}{\partial r})]$$

$$- T_1 \frac{\partial}{\partial r}(\rho_0v_0\phi_{5n}) + (\gamma-1)p_1 \frac{\partial}{\partial r}(v_0\phi_{5n}) \Big\} dr + \rho_0\phi_1[R'u_1$$

$$+ \frac{\beta}{\rho_wc_w} p_1 (\sqrt{1+R'^2} - 1)]_{r=R} = 0 \qquad (49)$$

3.4 Equations Describing the Wave Envelopes

Substituting the assumed solution, equations (19) and (20), into equation (49) yields the following 2N equations for the A's:

$$\sum_{n=1}^{2N} f_{mn} \frac{dA_n}{dx} = \sum_{n=1}^{2N} g_{mn}A_n \qquad (50)$$

where

$$f_{mn} = [\int_0^R \{\phi_{1m}(\rho_0\psi_n^u + u_0\psi_n^R) + \phi_{2m}(\rho_0u_0\psi_n^u) + \phi_{3m}(\rho_0u_0\psi_n^v$$

$$+ \phi_{4m}(\rho_0u_0\psi_n^w) + \phi_{5m}(\rho_0u_0\psi_n^T - (\gamma-1)u_0\psi_n^p)\}dr]e^{i\int k_n dx} \qquad (51)$$

$$g_{mn} = -\left[\int_0^R \left\{\phi_{1m}\left[\frac{\partial}{\partial x}(\rho_0\psi_n^u + u_0\psi_n^R)\right] - rv_0\psi_n^R\frac{\partial}{\partial r}\left(\frac{\phi_{1m}}{r}\right) + \phi_{2m}\left[\rho_0\frac{\partial}{\partial x}(u_0\psi_n^u) + \psi_n^R\left(u_0\frac{\partial u_0}{\partial x} + v_0\frac{\partial u_0}{\partial r}\right) + \frac{\partial\psi_n^p}{\partial x}\right] - \psi_n^u\frac{\partial}{\partial r}(\rho_0 v_0\phi_{2m}) + \phi_{3m}\left[\rho_0 u_0\frac{\partial\psi_n^v}{\partial x} + \rho_0\psi_n^u\frac{\partial v_0}{\partial x} + \psi_n^R\left(v_0\frac{\partial v_0}{\partial r} + u_0\frac{\partial v_0}{\partial x}\right)\right] - v_0\psi_n^v\frac{\partial}{\partial r}(\rho_0\phi_{3m}) + \phi_{4m}\left[\frac{\rho_0 v_0\psi_n^w}{r} + \rho_0 u_0\frac{\partial\psi_n^w}{\partial x}\right] - \psi_n^w\frac{\partial}{\partial r}(\rho_0 v_0\phi_{4m}) + \phi_{5m}\left[\rho_0 u_0\frac{\partial\psi_n^T}{\partial x} + \rho_0\psi_n^u\frac{\partial T_0}{\partial x} + \psi_n^R\left(v_0\frac{\partial T_0}{\partial r} + u_0\frac{\partial T_0}{\partial x}\right) - (\gamma-1)\times\left(u_0\frac{\partial\psi_n^p}{\partial x} + \psi_n^u\frac{\partial p_0}{\partial x} + \psi_n^v\frac{\partial p_0}{\partial r}\right)\right] - \psi_n^T\frac{\partial}{\partial r}(\rho_0 v_0\phi_{5m}) + (\gamma-1)\psi_m^p\frac{\partial}{\partial r}\times(v_0\phi_{5m}) + \phi_{1m}i(k_n - k_m)(\rho_0\psi_n^u + u_0\psi_n^R) + \phi_{2m}i(k_n - k_m)(\psi_n^p + \rho_0 u_0\psi_n^u) + \phi_{3m}i(k_n - k_m)\rho_0 u_0\psi_n^v + \phi_{4m}i(k_n - k_m)\rho_0 u_0\psi_n^w + \phi_{5m}i(k_n - k_m)u_0(\rho_0\psi_n^T - (\gamma-1)\psi_n^p)\right\}dr + \rho_0\phi_{1m}\left[R'\psi_n^u + \frac{\beta}{\rho_w c_w}\psi_n^p\left(\sqrt{1+R'^2} - 1\right)\right]_{r=R}\Bigg]e^{i\int k_n dx} \qquad (52)$$

For convenience the upstream modes are now denoted by A_n, $n = N+1,\ldots,2N$, i.e.,

$$A_{N+n} = \tilde{A}_n \qquad n = 1,2,3,\ldots,N$$

page 28
missing

4. NUMERICAL SOLUTION

A schematic drawing of the duct configuration under consideration is shown in Figure 1. The method of solution described can be applied to any type of circular duct, converging or diverging. For the purpose of demonstrating the method, a simple cosine variation of the duct radius is chosen.

$$R = 1 + a_2[-1 + \cos(2\pi\, x/L)] \tag{53}$$

The radius of the duct at the entrance has been chosen as the reference length, a_2 is a constant that specifies the magnitude of the variation in the outer wall (if $a_2 = 0$, the duct is uniform), and L is the dimensionless length of the duct. The entire length of the duct is assumed to be lined with a point-reacting liner consisting of a thin porous facing sheet backed by cellular cavities of depth d; if the facing sheet is thin and the cavity depth is small, the specific acoustic admittance is described by

$$\beta = \frac{1}{R_e(1 - i\omega/\omega_0) + i\cot(\omega d/T_w^{1/2})} \tag{54}$$

where R_e is the flow resistance and ω_0 is the characteristic frequency of the facing sheet. Thus, the physical characteristics of the duct are prescribed by input of the values of a_2, L, R_e, ω_0 and d to the program.

A simple model of the mean flow has been selected for the preliminary stages of the application of the theory. This model uses one-dimensional gas dynamics theory to describe the mean-flow variables in the inviscid core; the velocity profile in the boundary layer is taken to be a quarter-sine profile, that is

$$\frac{u_0}{u_c} = \sin[\pi(R - r)/2\delta] \quad r \geq R - \delta$$
$$= 1 \quad r \leq R - \delta \tag{55}$$

The temperature profile is related to the velocity profile by[51]

$$\frac{T_0}{T_c} = 1 + r_1 \frac{\gamma-1}{2} M_c^2[1 - (\frac{u_0}{u_c})^2] + \frac{T_w - T_{ad}}{T_c}[1 - \frac{u_0}{u_c}] \tag{56a}$$

$$T_{ad}/T_c = 1 + r_1 \frac{\gamma-1}{2} M_c^2 \tag{56b}$$

where the subscript c refers to values in the inviscid core, T_w is the wall temperature, T_{ad} is the adiabatic wall temperature, δ is the boundary-layer thickness, r_1 is the recovery factor and $\gamma = 1.4$ is the ratio of the gas specific heats. The axial variation of the boundary-layer displacement thickness δ^* is assumed to be known and is specified in the program by a simple polynomial variation:

$$\delta^*/\delta_0^* = 1 + b_1(x/L) + b_2(x/L)^2$$

The displacement thickness and the Mach number within the uniform core have prescribed values δ_0^* and M_{c_0}, at $x = 0$; the subsequent axial variation of δ and M_c are calculated within the program from the definition of displacement thickness and from mass-flow considerations. The one-dimensional gas-dynamics theory provides the axial variation of T_c, ρ_c, u_c, etc. and the boundary layer profiles are computed from equations (55) and (56). Thus, the mean flow within the duct is prescribed by input of the values of M_{c_0}, δ_0^*, b_1, b_2, r_1, γ, and T_w to the program.

To calculate the changes in the amplitude of the acoustic wave first requires the eigenfunctions ψ_n. The quasi-parallel flow equations (29) and (30) are solved by using a Runge-Kutta forward-integration technique and by employing a Newton-Raphson procedure to determine the eigenvalue k.

To determine the coefficients q_{mn} of equation (52), one has to evaluate the axial gradients of the wavenumber, k, and of the eigenfunctions ψ_n. These axial derivatives can be obtained from equations (29) and (30); these two equations are written in the form

$$\hat{\omega}^2 \mathcal{L}(\psi^p) = \frac{\partial^2 \psi^p}{\partial r^2} + \left[\frac{1}{r} + \frac{T_0'}{T_0} + \frac{2ku_0'}{\hat{\omega}}\right]\frac{\partial \psi^p}{\partial r} + \left[\frac{\hat{\omega}^2}{T_0} - k^2 - \frac{m^2}{r^2}\right]\psi^p = 0 \tag{57}$$

$$\frac{\partial \psi^p}{\partial r} - \frac{i\omega\beta\psi^p}{T_w^{1/2}} = 0 \quad \text{at } r = R \tag{58}$$

Differentiating the above equations with respect to x and using $\mathcal{L}(\psi^p) = 0$, one obtains

$$\begin{aligned}\hat{\omega}^2 \mathcal{L}\left(\frac{\partial \psi^p}{\partial x}\right) = &- \left[\frac{1}{T_0}\frac{\partial^2 T_0}{\partial r \partial x} - \frac{1}{T_0^2}\frac{\partial T_0}{\partial x}\frac{\partial T_0}{\partial r} + \frac{2}{\hat{\omega}}\frac{\partial u_0}{\partial r}\frac{dk}{dx} + \frac{2k}{\hat{\omega}}\frac{\partial^2 u_0}{\partial r \partial x}\right. \\ &\left. + \frac{2k}{\hat{\omega}^2}\frac{\partial u_0}{\partial r}\left(u_0\frac{dk}{dx} + k\frac{\partial u_0}{\partial x}\right)\right]\frac{\partial \psi^p}{\partial r} + \left[\frac{2\hat{\omega}}{T_0}\left(u_0\frac{dk}{dx} + k\frac{\partial u_0}{\partial x}\right)\right. \\ &\left. + \frac{\hat{\omega}^2}{T_0^2}\frac{\partial T_0}{\partial x} + 2k\frac{dk}{dx}\right]\psi^p\end{aligned} \tag{59}$$

$$\begin{aligned}\frac{\partial}{\partial r}\left(\frac{\partial \psi^p}{\partial x}\right) - i\frac{\omega}{T_w^{1/2}}\beta\frac{\partial \psi^p}{\partial x} = &- R'\left(\frac{\partial^2 \psi^p}{\partial r^2} - i\frac{\omega}{T_w^{1/2}}\beta\frac{\partial \psi^p}{\partial r}\right) \\ &+ \frac{i\omega}{T_w^{1/2}}\frac{d\beta}{dx}\psi^p - \frac{1}{2}\frac{i\omega}{T_w^{3/2}}\frac{dT_w}{dx}\beta\psi^p \quad \text{at } r = R\end{aligned} \tag{60}$$

Thus, equation (59) can be written as

$$\mathcal{L}\left(\frac{\partial \psi^p}{\partial x}\right) = \zeta_1(x,r)\frac{dk}{dx} + \zeta_2(x,r) \tag{61}$$

where

$$\zeta_1 = \frac{2}{\hat{\omega}^2}\left(\frac{u_0\hat{\omega}}{T_0} + k\right)\psi^p - \frac{2}{\hat{\omega}^4}\frac{\partial u_0}{\partial r}\left(\hat{\omega} + u_0 k\right)\frac{\partial \psi^p}{\partial r} \tag{62}$$

$$\zeta_2 = \frac{1}{T_0}\left[\frac{2}{\hat{\omega}}\, k\, \frac{\partial u_0}{\partial x} + \frac{1}{T_0}\frac{\partial T_0}{\partial x}\right]\psi^p + \frac{1}{\hat{\omega}^2}\left[-\frac{\partial}{\partial x}\left(\frac{1}{T_0}\frac{\partial T_0}{\partial r}\right)\right.$$

$$\left. - 2\,\frac{k}{\hat{\omega}}\left(\frac{\partial^2 u_0}{\partial r \partial x} + \frac{k}{\hat{\omega}}\frac{\partial u_0}{\partial r}\frac{\partial u_0}{\partial x}\right)\right]\frac{\partial \psi^p}{\partial r} \qquad (63)$$

Equations (60) - (61) will have a solution for $\frac{\partial \psi^p}{\partial x}$ if, and only if, a solvability condition is satisfied. To determine the solvability condition, one multiplies equation (61) by $r\psi^p$, integrates from r = 0 to r = R, and obtains

$$\frac{dk}{dx}\int_0^R \zeta_1 r\psi^p dr = -\int_0^R \zeta_2 r\psi^p dr + \frac{RT_w}{\omega^2}\psi^p\left[-R'\left(\frac{\partial^2\psi^p}{\partial r^2} - \frac{i\omega}{T_w^{1/2}}\,\beta\,\frac{\partial \psi^p}{\partial r}\right.\right.$$

$$\left.\left. + \left(\frac{i\omega}{T_w^{1/2}}\frac{d\beta}{dx} - \frac{1}{2}\frac{i\omega}{T_w^{3/2}}\frac{dT_w}{dx}\,\beta\right)\psi^p\right]\right|_{r=R} \qquad (64)$$

The integrals in equation (64) are evaluated numerically by using Simpson's rule, and the value of $\frac{dk}{dx}$ is thus determined. With $\frac{dk}{dx}$ known, equation (61) can be integrated by letting

$$\frac{\partial \psi^p}{\partial x} = \psi^p(r;x)E(r;x) \qquad (65)$$

and solving for E(r;x).

The number of radial modes to be considered and the values for their propagation constants at x = 0 must be supplied as input to the program. The propagation constants at each subsequent axial station are estimated from k and $\frac{dk}{dx}$ at the previous station and the usual iteration procedure is used to obtain convergence. This helps to reduce the time required for the calculation and avoids the usual jumps encountered between the modes.

The adjoint functions are found by using the relations (39) - (43) from the quasi-parallel-flow variables ψ^p, $\frac{\partial \psi^p}{\partial x}$, and k. The coefficients f_{mn} and g_{mn} are then evaluated from equations (51) and (52). Writing equation (50) in matrix form, FdA/dx = GA, and solving for dA/dx, one obtains

$$\frac{dA}{dx} = F^{-1}GA \tag{66}$$

where A is a column matrix whose elements are the A_n.

A Runge-Kutta forward-integration technique is used to solve equations (66) for the function A at each axial station. Since the problem is linear, one can determine the solution for any problem subject to general boundary conditions at the two ends of the duct by a linear combination of 2N linearly independent solutions.

The linearly independent solutions are obtained by setting all mode amplitudes except one to zero at x = 0 and integrating equation (66) to x = L. One such integration for each of the 2N modes allows one to obtain the transfer matrices TR_1, TR_2, TR_3, TR_4 which are defined by

$$\begin{aligned} B^+(L) &= TR_1B^+(0) + TR_2B^-(0) \\ B^-(L) &= TR_3B^+(0) + TR_4B^-(0) \end{aligned} \tag{67}$$

where $B^+(x)$ is a column vector of the amplitudes $A_n e^{i\int k_n dx}$ of the right-running modes and $B^-(x)$ is a column vector of the amplitudes $\tilde{A}_n e^{i\int \tilde{k}_n dx}$ of the left-running modes. Following Reference 55, results are obtained in the form of transmission and reflection coefficients for the variable-area segment being considered. The transmission and reflection coefficients relate the magnitudes of the outgoing modes to those of the incoming modes,

$$B^{+}(L) = T^{L,0}B^{+}(0) + R^{L,L}B^{-}(L)$$

$$B^{-}(0) = T^{0,L}B^{-}(L) + R^{0,0}B^{+}(0) \tag{68}$$

and are calculated from the transfer matrices by[50]

$$\left.\begin{aligned} T^{0,L} &= TR_4^{-1} \\ R^{0,0} &= -TR_4^{-1}TR_3 \\ R^{L,L} &= TR_2TR_4^{-1} \\ T^{L,0} &= TR_1 + TR_2R^{0,0} \end{aligned}\right\} \tag{69}$$

[The reflection coefficients are the negative of those defined in reference 55 as a consequence of the use of the positive sign on the $\tilde{\psi}_n^p$ term in equation (19)]. The (m,n) term of $T^{L,0}$ represents the transmission of the m^{th} radial mode at x = L due to the n^{th} radial mode incident at x = 0, etc.

5. DISCUSSION

The computer program described in the previous section has been used to investigate the effect of a compressible mean flow on the multimodal wave propagation in a nonuniform circular duct. There exist no numerical or experimental results for this problem that can be used for comparison purposes. However, as stated in the method of solution, the present solution recovers that based on the method of multiple scales if the axial variations are slow. Moreover, calculations made for a uniform duct with a fully developed boundary layer agree with the well-known results for waves propagating in a uniform duct.

In all the cases reported here, the coefficient a_2 was chosen to be 0.12 and the duct length L to be 2. This gives a maximum wall slope of 0.37, sufficiently large to produce modal coupling but not so large as to entirely negate the validity of the mean flow model. The boundary-layer displacement thickness at the entrance is $\delta_0^* = 0.02$ and it is assumed that it decreases linearly in the converging duct section $0 \leq x \leq 1$ with $b_1 = -1$ and $b_2 = 0$; although this is artificial, it serves to illustrate the applicability of the method. The circumferential mode number is zero in all the reported calculations. The recovery factor for the mean temperature profile is assumed to be unity. The calculations are terminated at the minimum cross section of the duct at $x = 1$ in all cases. Thus, the transmission and reflection coefficients presented are for a converging duct for downstream propagating modes and a diverging duct for the upstream-propagating modes. In all lined-duct cases, the liner properties are $R_e = 0.8$, $\omega_0 = 15$, $d = .05$.

In Figure 2, the axial variations of the functions A_1 and $A_1\exp(i\int k_1 dx)$ have been plotted. It can be seen that the function A_1 varies more slowly than the mode amplitude $A_1\exp(i\int k_1 dx)$. As noted earlier, this is the basic advantage of the wave-envelope technique, since fewer numerical steps are required to describe the more slowly-varying curve. The wave envelope technique becomes more advantageous as the duct length and the frequency are increased. Figure 3 shows the results for a higher frequency. Clearly, as the wavelength of the signal decreases further, a direct numerical calculation of the amplitude $A_n\exp(\int ik_n dx)$ becomes more difficult.

In Figures 4 and 5, the strength of the interaction among the modes is demonstrated. In Figure 4, the first right-running mode is incident at the entrance of the duct with an amplitude (1.0 + 0.0i). As this mode propagates through the duct the second right-running mode develops and starts propagating with an amplitude that is small compared with the incident mode. Although the left-running modes also develop, they are insignificant throughout the duct indicating that reflection effects are very small. It was reported by Kaiser and Nayfeh[50] that reflection is insignificant for the case of no mean flow except near cut off; the results shown in Figure 4 are consistent with this general conclusion. However, in some cases with mean flow, such as the one shown in Figure 5, a significant development of left-running modes may occur. Thus, both sets of modes must be included for determining the propagation in lined ducts with flow.

In Figure 6, the axial variation of the absolute value of the amplitude $A_n\exp[\int ik_n dx]$ for the left-running modes has been plotted. It can be seen that as the Mach number approaches unity, the amplitudes

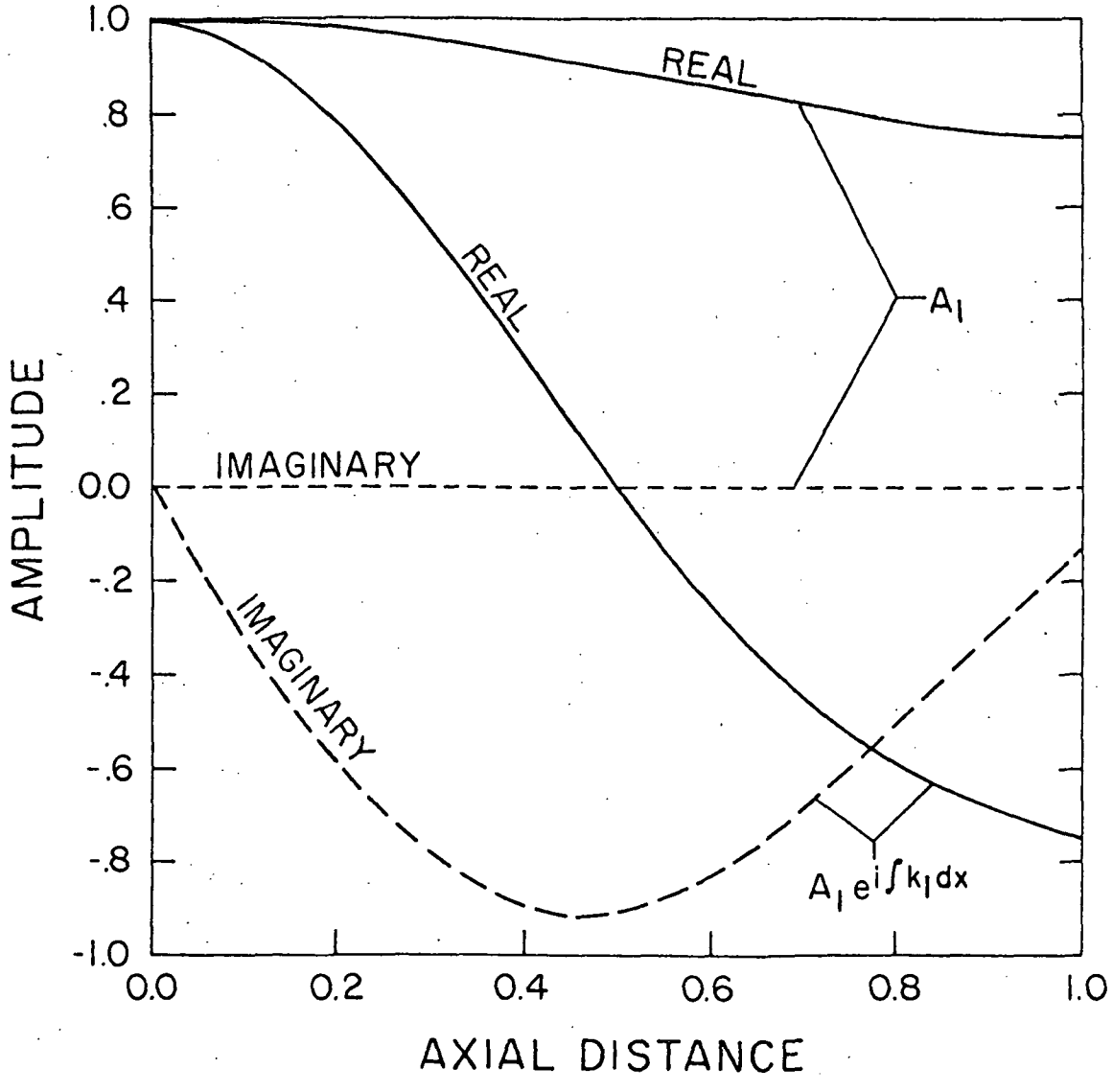

Figure 2. Comparison between the slowly varying function A_1 and $A_1\exp(i\int k_1 dx)$ in a lined duct; first right-running mode incident at x = 0; $\omega = 4$, N = 1, $M_{C_0} = 0.3$.

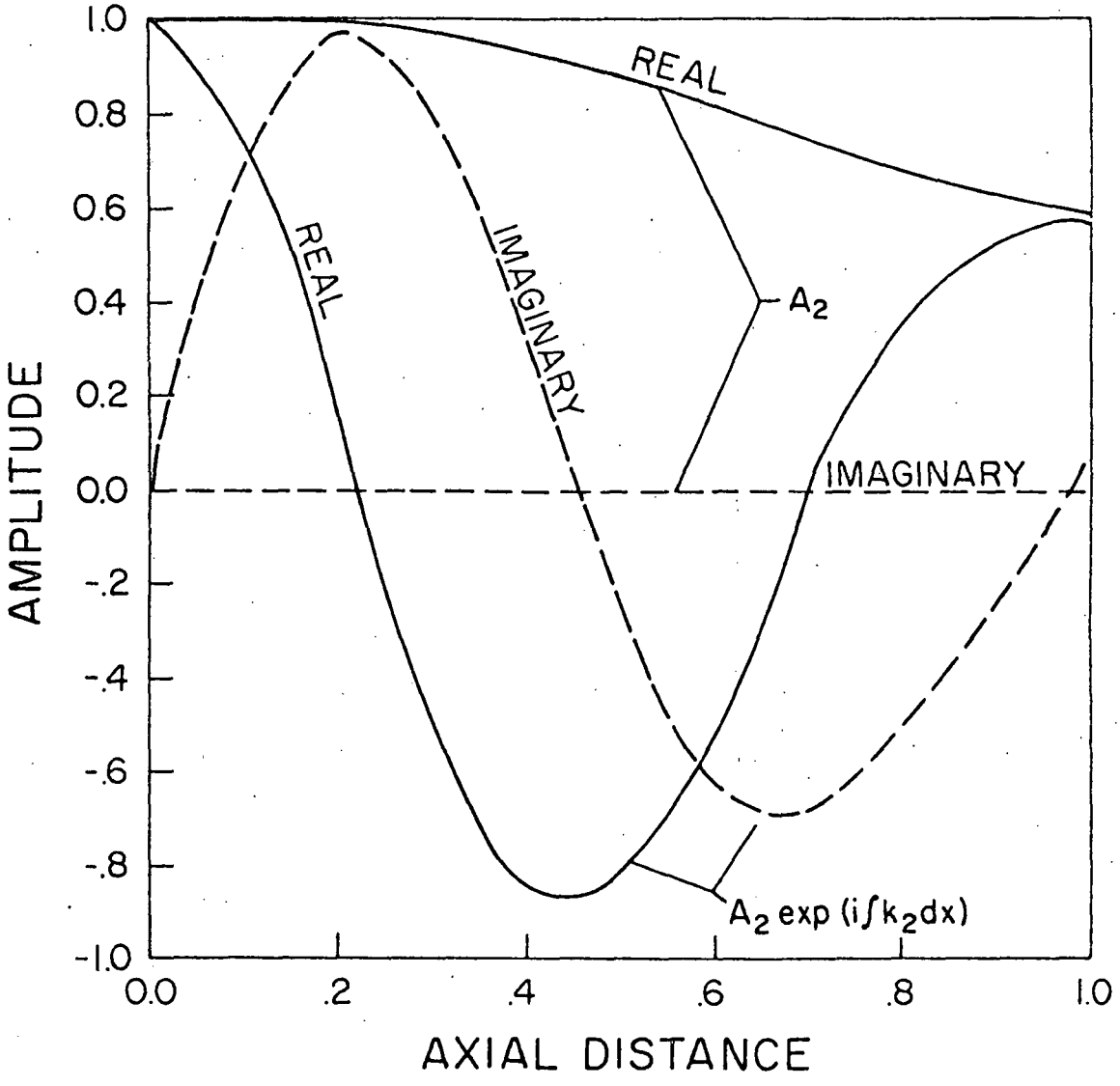

Figure 3. Comparison between the slowly-varying function A_2 and $A_2\exp(i\int k_2 dx)$ in a lined duct; second right-running mode incident at x = 0; ω = 10, N = 3, M_{C_0} = 0.3.

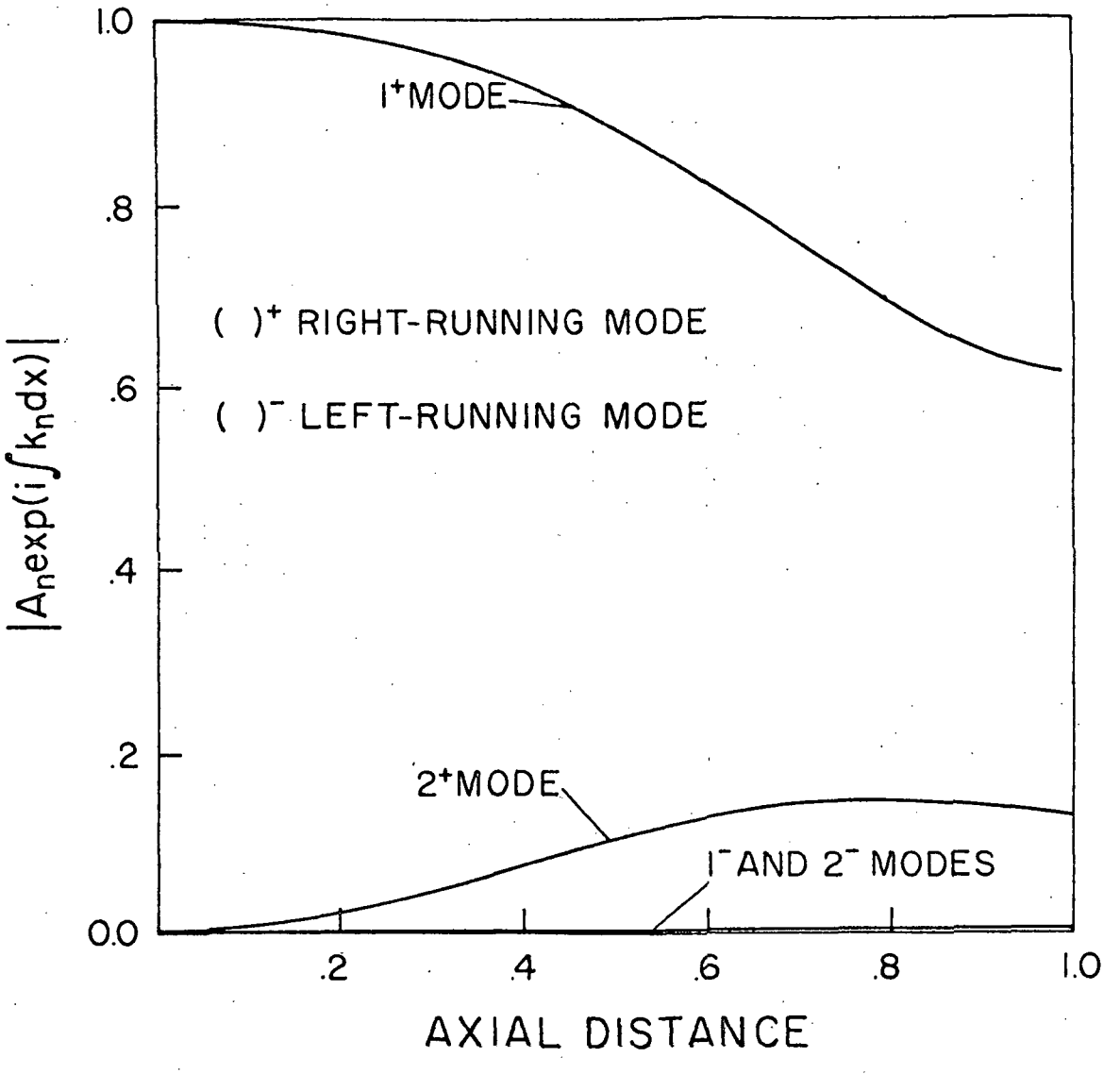

Figure 4. The absolute value of mode amplitudes in a hard-wall duct; first right-running mode incident at x = 0; $\omega = 7$, N = 2, $M_{c_0} = 0.36$, $M_t = 0.86$ where M_t is the throat Mach number (at x = 1.0).

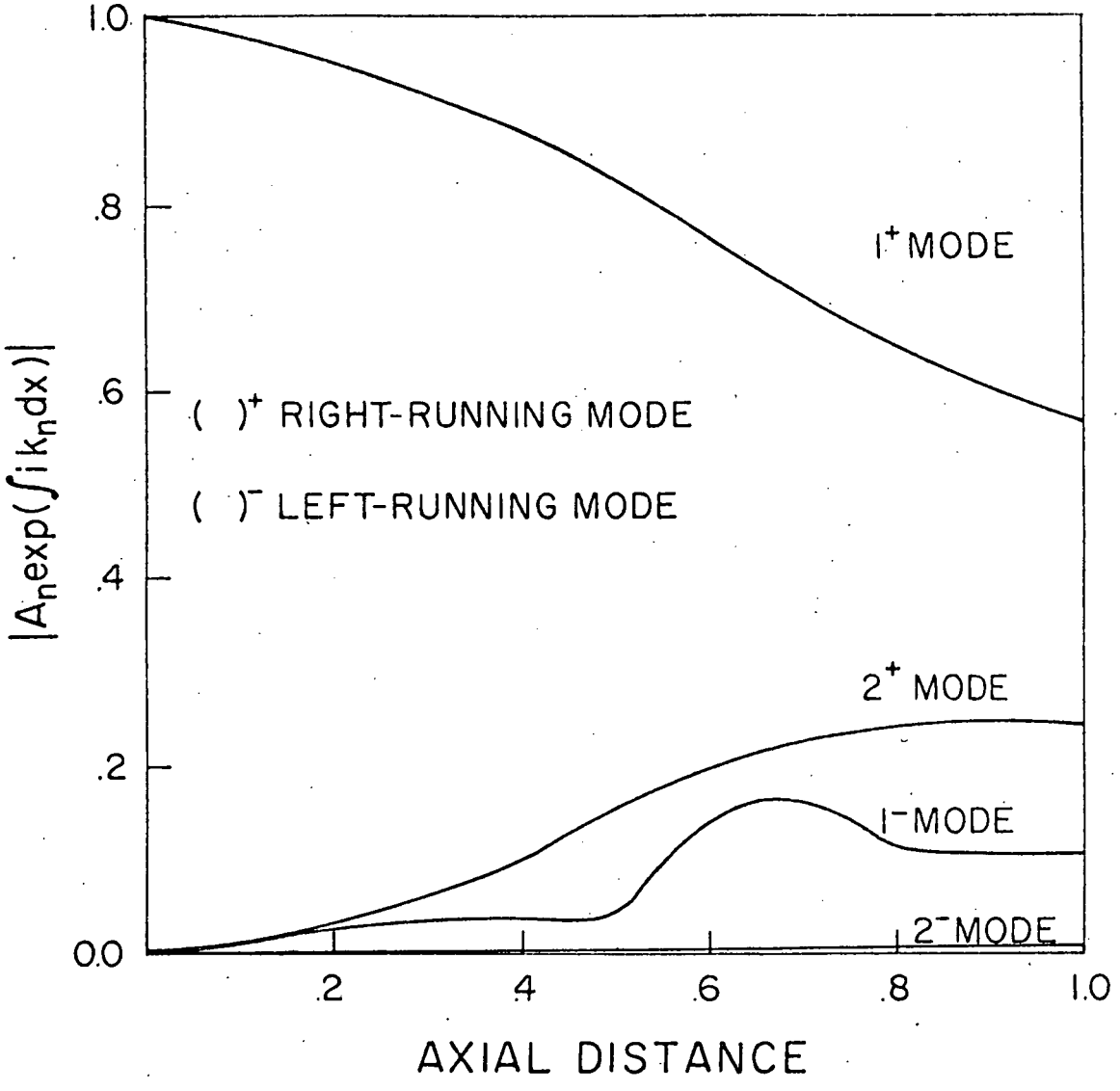

Figure 5. The absolute value of mode amplitudes in a lined duct; first right-running mode incident at x = 0; $\omega = 7$, N = 2, $M_{c_0} = 0.3$, $M_t = 0.6$.

become very large. This is to be expected because the wavenumbers of the left-running modes become very large. This can be seen more easily from an examination of the wavenumbers for the case of uniform flow; that is

$$k = -\frac{M_c\omega \mp \sqrt{\omega^2 - (1 - M_c^2)\kappa^2}}{1 - M_c^2}$$

where M_c is the Mach number and κ is the eigenvalue. As $M_c \to 1$, one of the values of k approaches infinity, while the other remains bounded. This unusual behavior of the solution is due to the linearization of the acoustic equations. Thus, the inclusion of nonlinear terms becomes necessary at high Mach numbers. Although the numerical results may qualitatively show the correct behavior for cases in which M_c is greater than about 0.75, they are quantitatively in error because the linearized theory is not valid at these high Mach numbers. Thus, Figure 6 shows qualitatively that the amplitude of an incident mode at x = L must be very large for its amplitude at x = 0 to be non-negligible. Consequently, the transmission and reflection coefficients for such modes will be small.

Figures 7 and 8 show the variation of the transmission coefficients at x = 0 due to modes incident at x = L with throat Mach number for hard and soft-walled ducts, respectively. In this case, the transmission coefficients represent waves propagating against the mean flow. The direct transmission coefficients decrease rapidly with increasing throat Mach number. The effect of the axial variations is evident in these figures which show the coupling of the modes. However, the intermodal transmission coefficients are small compared with the direct transmission coefficients except for throat Mach numbers larger than 0.75. This is

perhaps expected because, although the axial variations are not small, they are not very large; the maximum wall slope in all cases is 0.37. Figure 7 shows also that the intermodal transmission coefficient T_{12} from the high to the low mode is smaller than the intermodal transmission coefficient T_{21} from the low to the high mode. Comparing Figures 7 and 8 shows as expeced that the overall direct transmisssion coefficients for the sofl-walled case are smaller than those for the hard-walled case. Moreover, the intermodal transmission coefficients decrease when the walls are lined.

The transmission coefficients at x = L for modes incident at x = 0 are plotted in Figure 9 for a hard-walled duct. In this case, the transmission coefficients represent waves propagating with the flow. It indicates that the amplitudes of the transmitted modes in a converging duct decrease with increasing throat Mach number. Higher throat Mach numbers tend to decrease the coefficients of the direct transmitted modes more than the intermodal coefficients. As in the case of upstream propagation, Figure 9 indicates that the intermodal coupling is more effective from the lower to the higher-order modes. Comparing Figures 9 and 10 indicates that lining the duct walls leads to a quantitative reduction in the direct transmission coefficients without any significant qualitative change. The intermodal coefficients seem not to be affected significantly by the throat Mach number or the wall liner. Figures 11, 12, and 13 present the transmission coefficients at $\omega = 10$ in a lined duct for the first, second, and third upstream modes, respectively, including the intermodal coupling. In most cases an increase in Mach number reduces the magnitude of the transmitted mode; however,

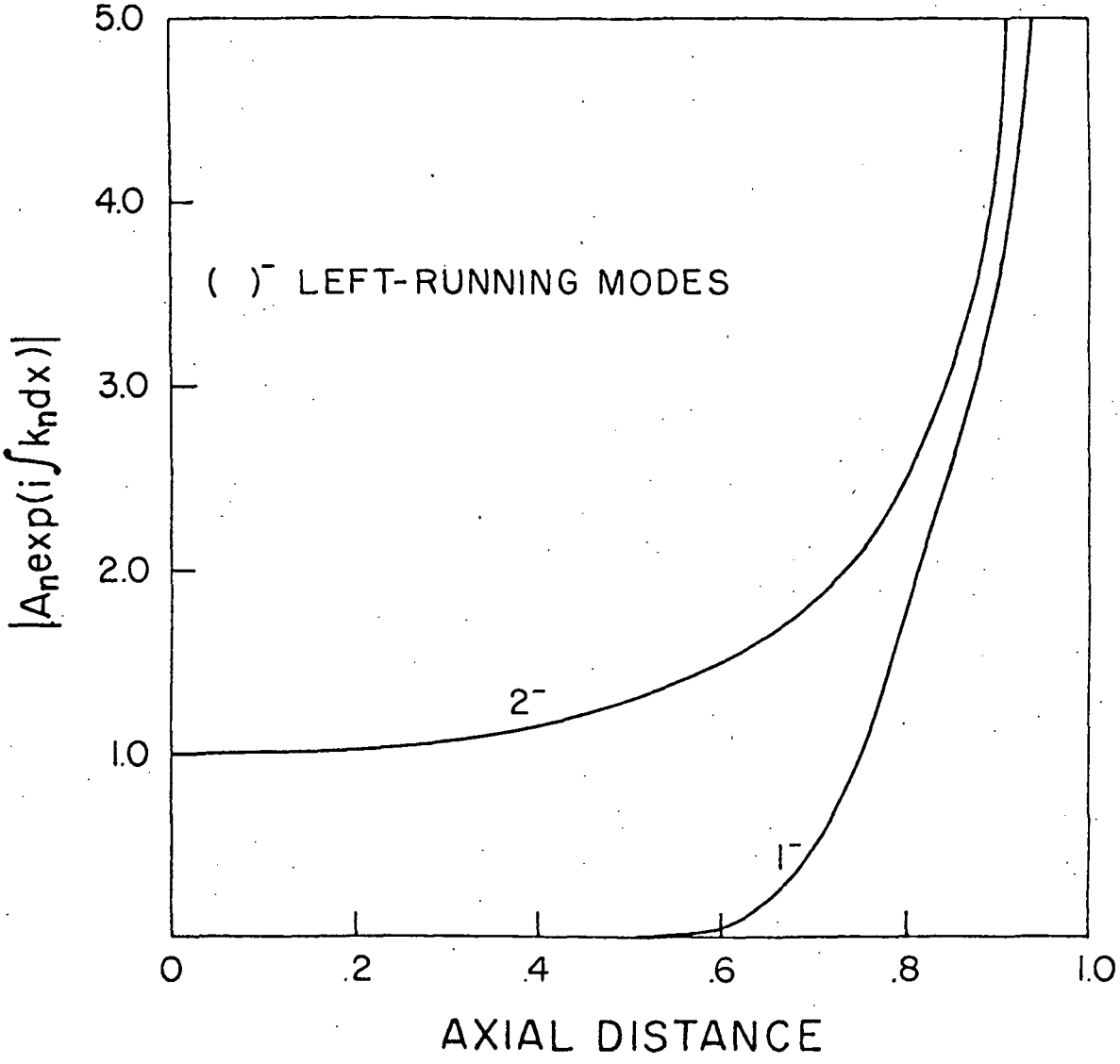

Figure 6. The absolute value of mode amplitudes in a lined duct; second left-running mode transmitted at x = 0; $\omega = 7$, $N = 2$, $M_{c_0} = 0.364$, $M_t = 0.95$.

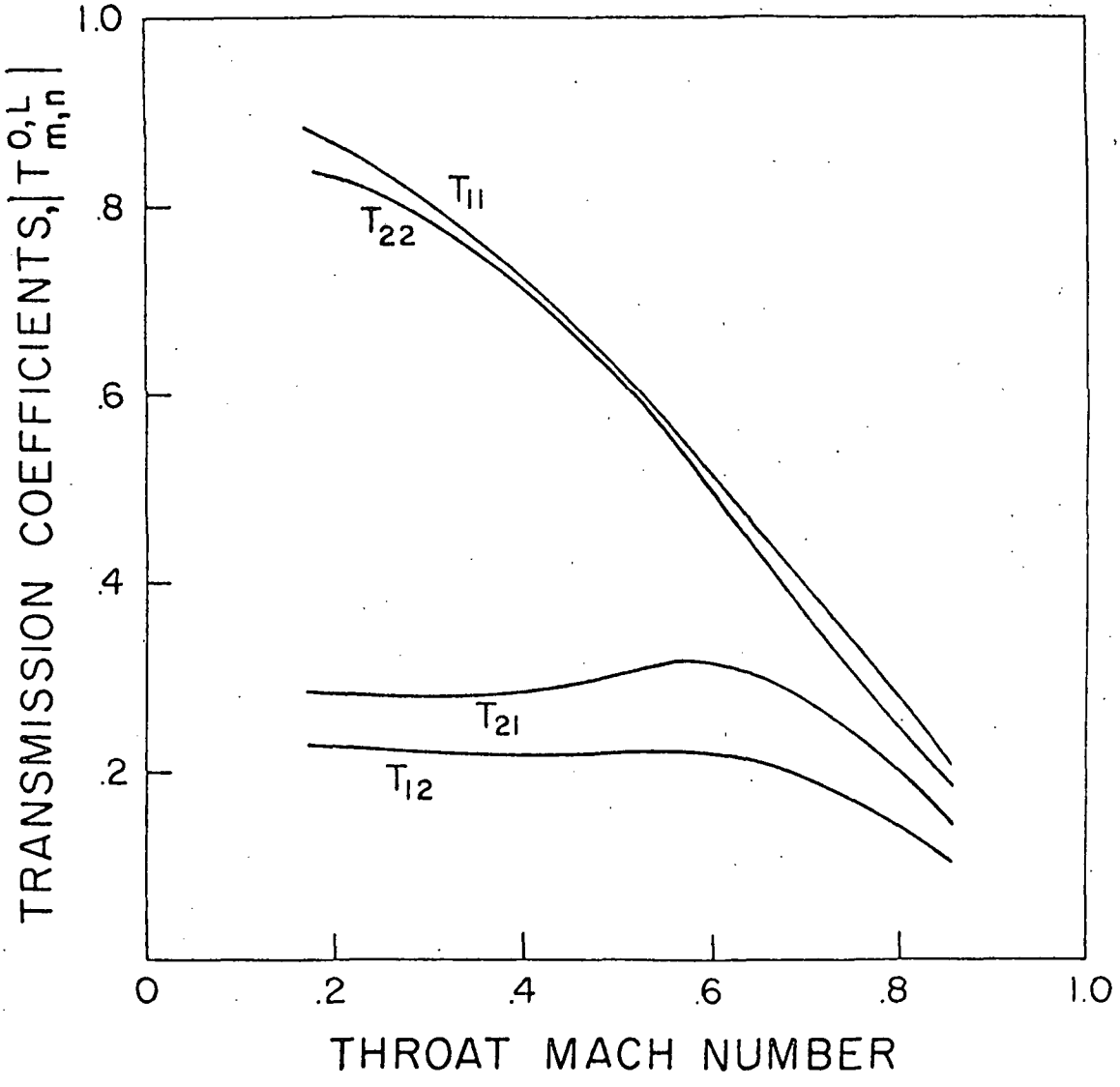

Figure 7. Effect of the throat Mach number on the absolute value of the transmission coefficients in a hard-wall duct; left-running modes incident at x = 1.0; ω = 7, N = 2.

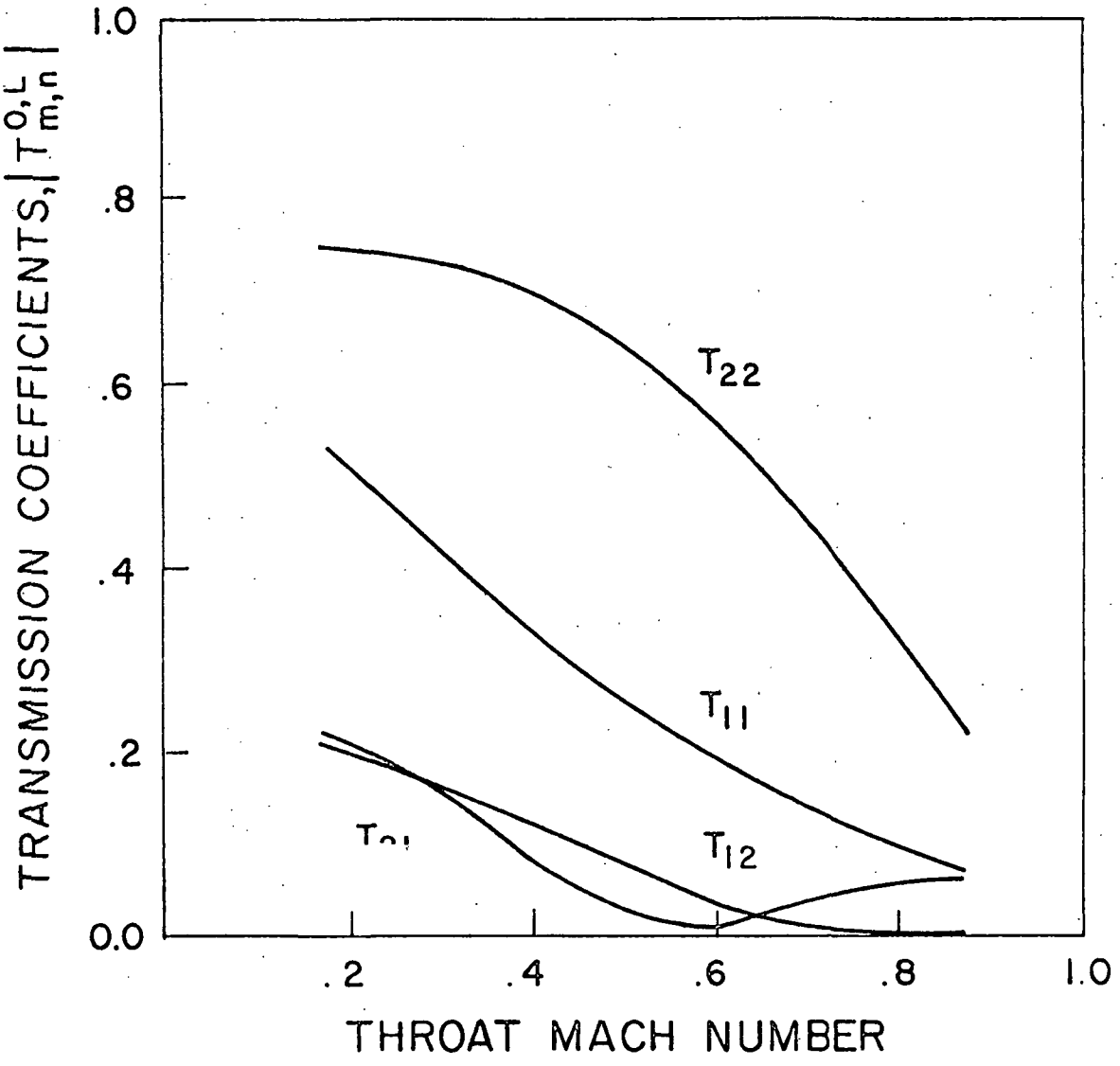

Figure 8. Effect of the throat Mach number on the absolute value of the transmission coefficients in a lined duct; left-running modes incident at x = 1.0; ω = 7, N = 2.

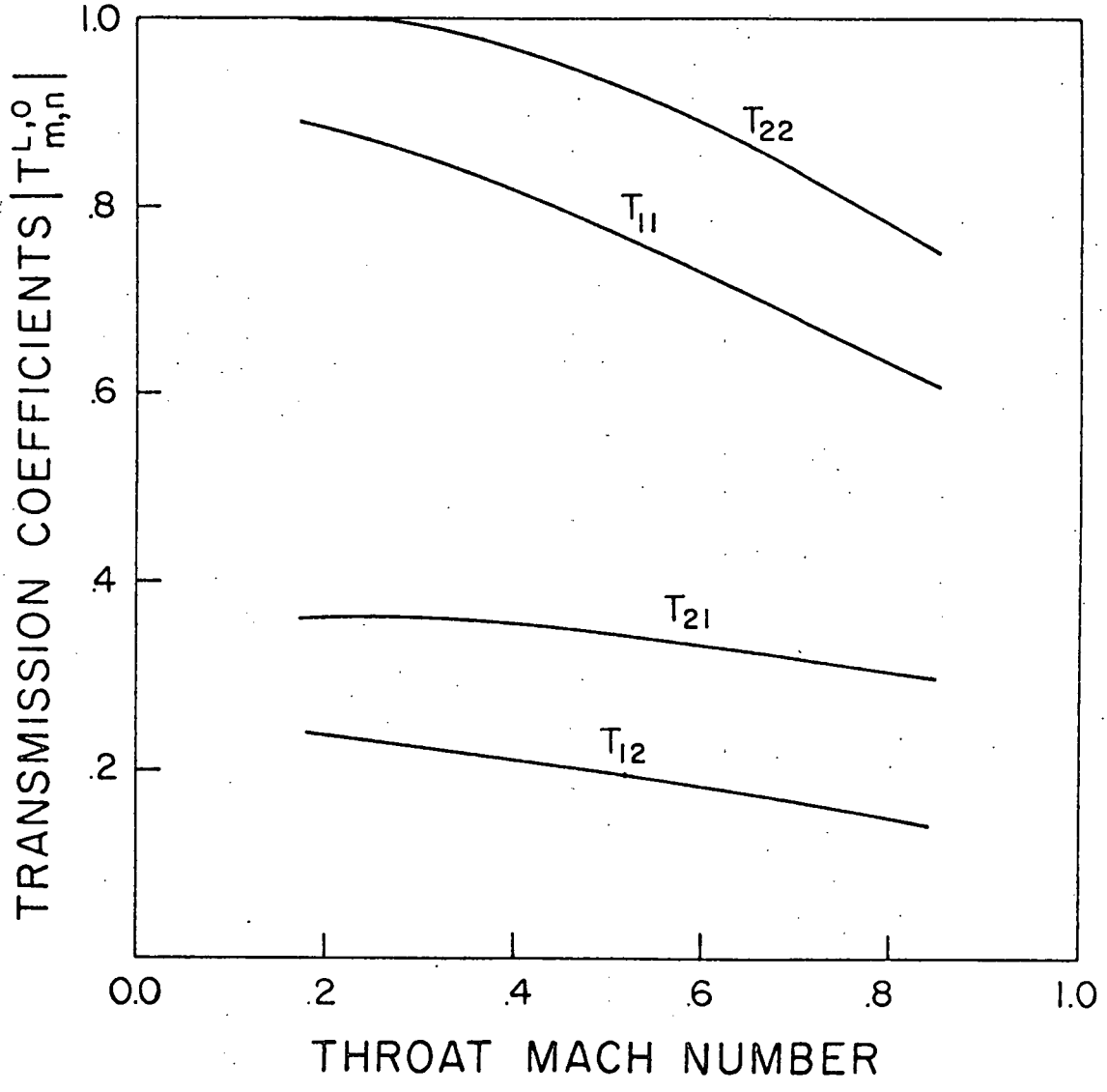

Figure 9. Effect of the throat Mach number on the absolute value of the transmission coefficients in a hard-wall duct: right-running modes incidents at $x = 0$; $\omega = 7$, $N = 2$.

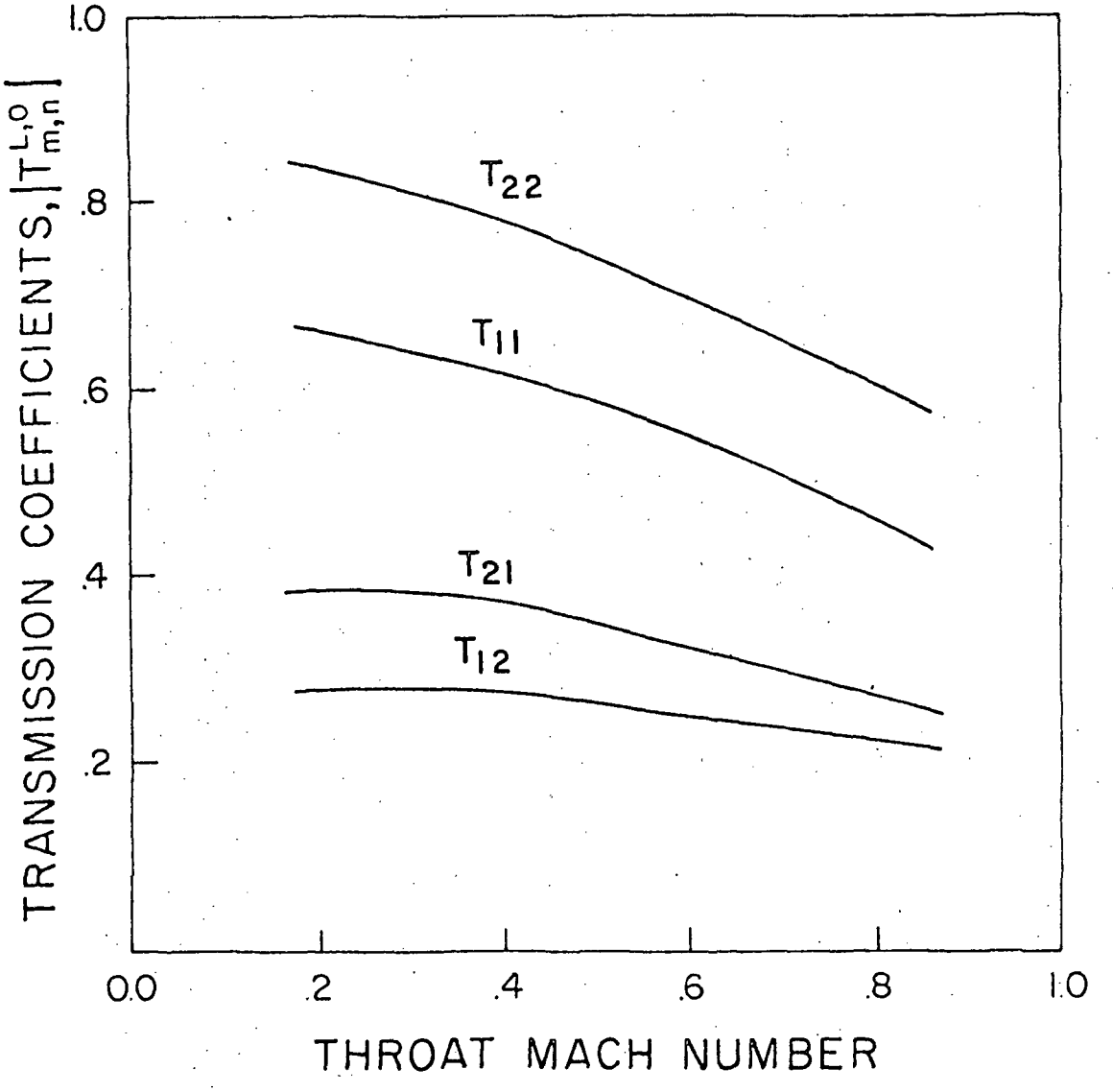

Figure 10. Effect of the throat Mach number on the absolute value of the transmission coefficients in a lined duct; right-running modes incident at $x = 0$; $\omega = 7$, $N = 2$.

the direct transmission of the third mode (T_{33}) and the transmission of the first mode due to the input of the second (T_{12}) increase with increasing Mach number up to $M_t \sim 0.5 - 0.7$ before decreasing at high Mach numbers.

Figures 14 and 15 show the variation of the reflection coefficients at the left end for hard and soft-walled ducts, respectively. For the hard-walled case, the direct and intermodal reflection coefficients are insignificant even compared with the intermodal transmission coefficients shown in Figures 9 and 10. Comparing Figure 14 and 15 indicates that the reflection coefficients depend strongly on the wall lining and throat Mach number. A rather abrupt increase in the magnitude of the reflection of the downstream propagating waves into the lowest upstream mode occurs at a throat Mach number of ~ 0.4. Reflection into the second upstream mode and all reflections at $x = 1.0$ (not shown) remain small even in the lined-duct case.

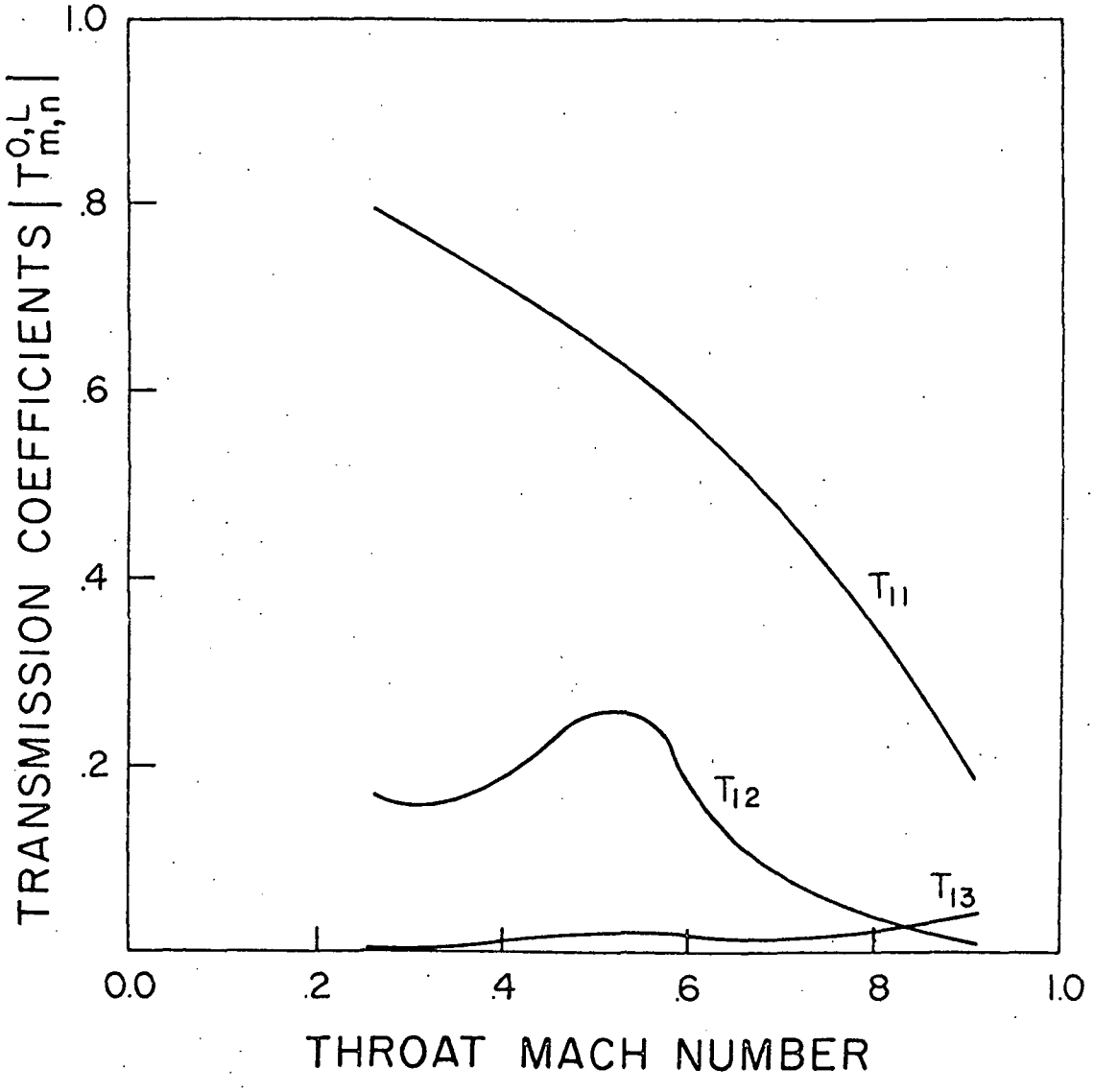

Figure 11. Effect of the throat Mach number on the absolute value of the transmission of the first left-running mode in a lined duct; $\omega = 10$, $N = 3$.

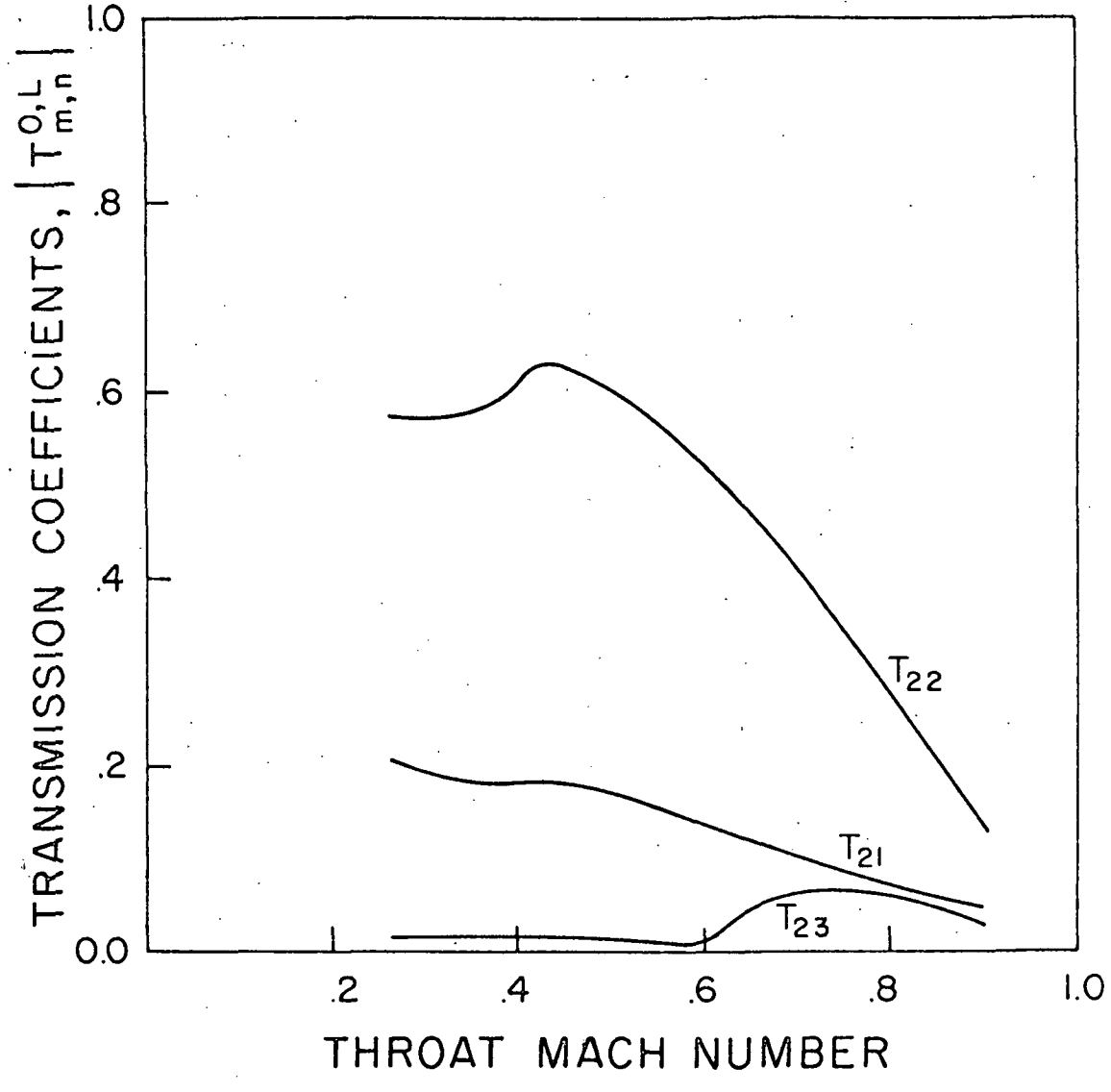

Figure 12. Effect of the throat Mach number on the absolute value of the transmission of the second left-running mode in a lined duct; $\omega = 10$, $N = 3$.

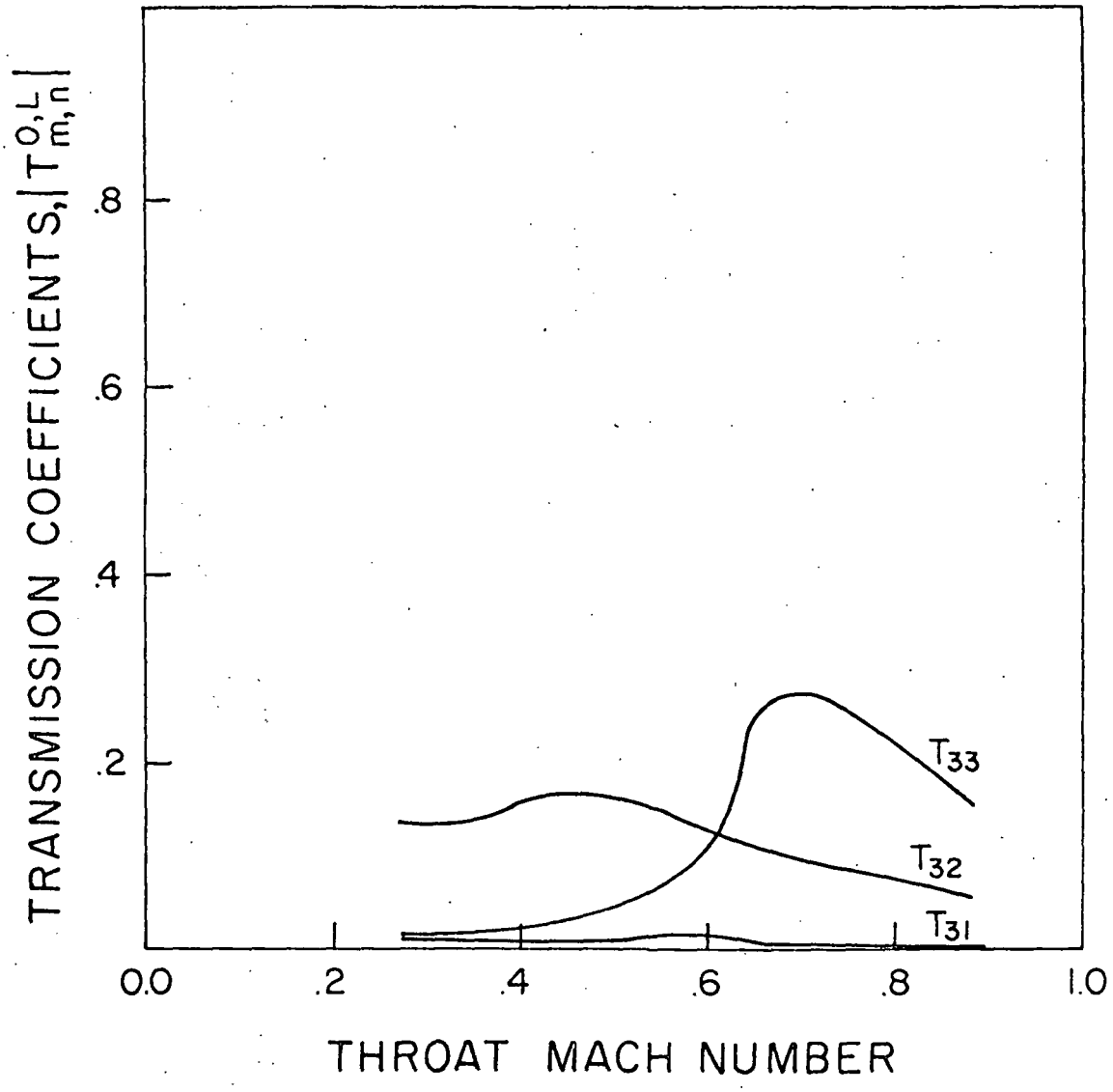

Figure 13. Effect of the throat Mach number on the absolute value of the transmission of the third left-running mode in a lined duct; $\omega = 10$, $N = 3$.

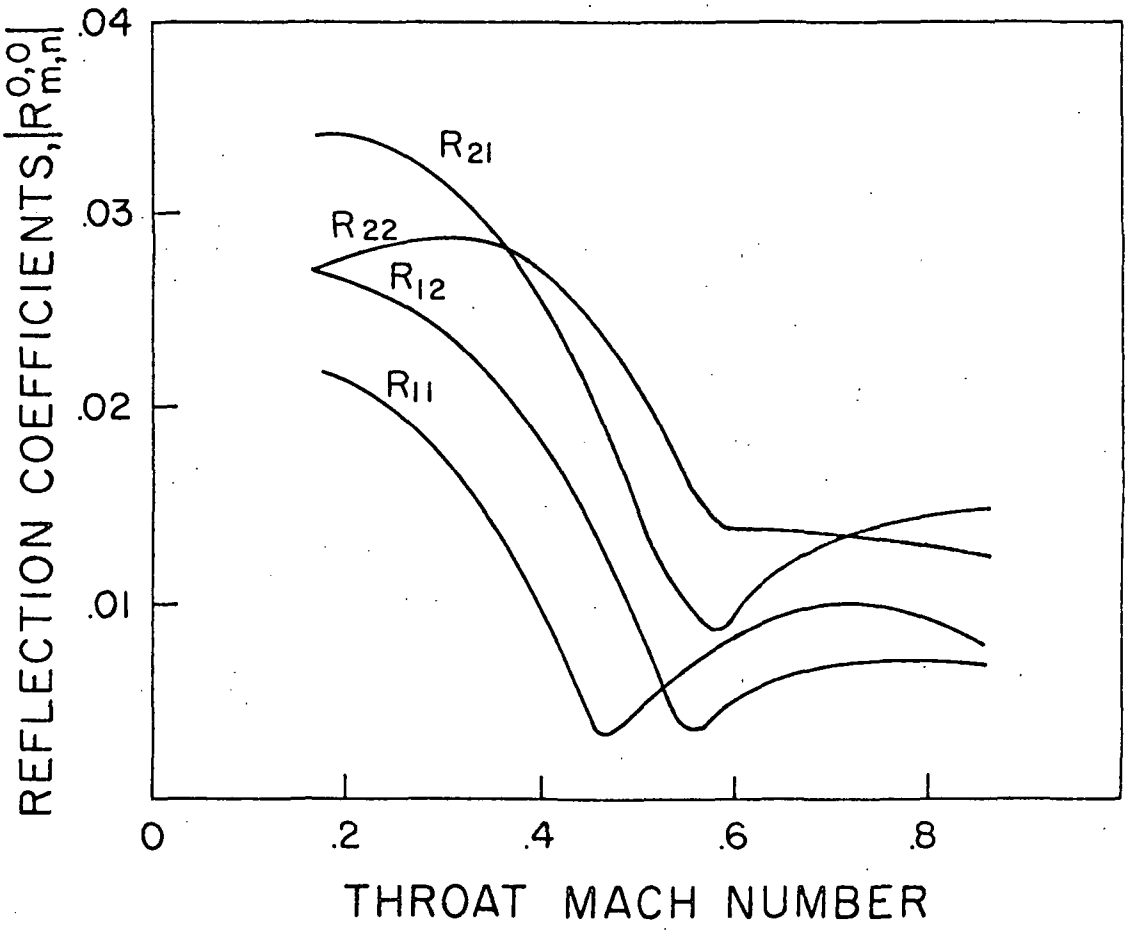

Figure 14. Effect of the throat Mach number on the absolute value of the reflection coefficients in a hard-wall duct; right-running modes incident at x = 0; ω = 7, N = 2.

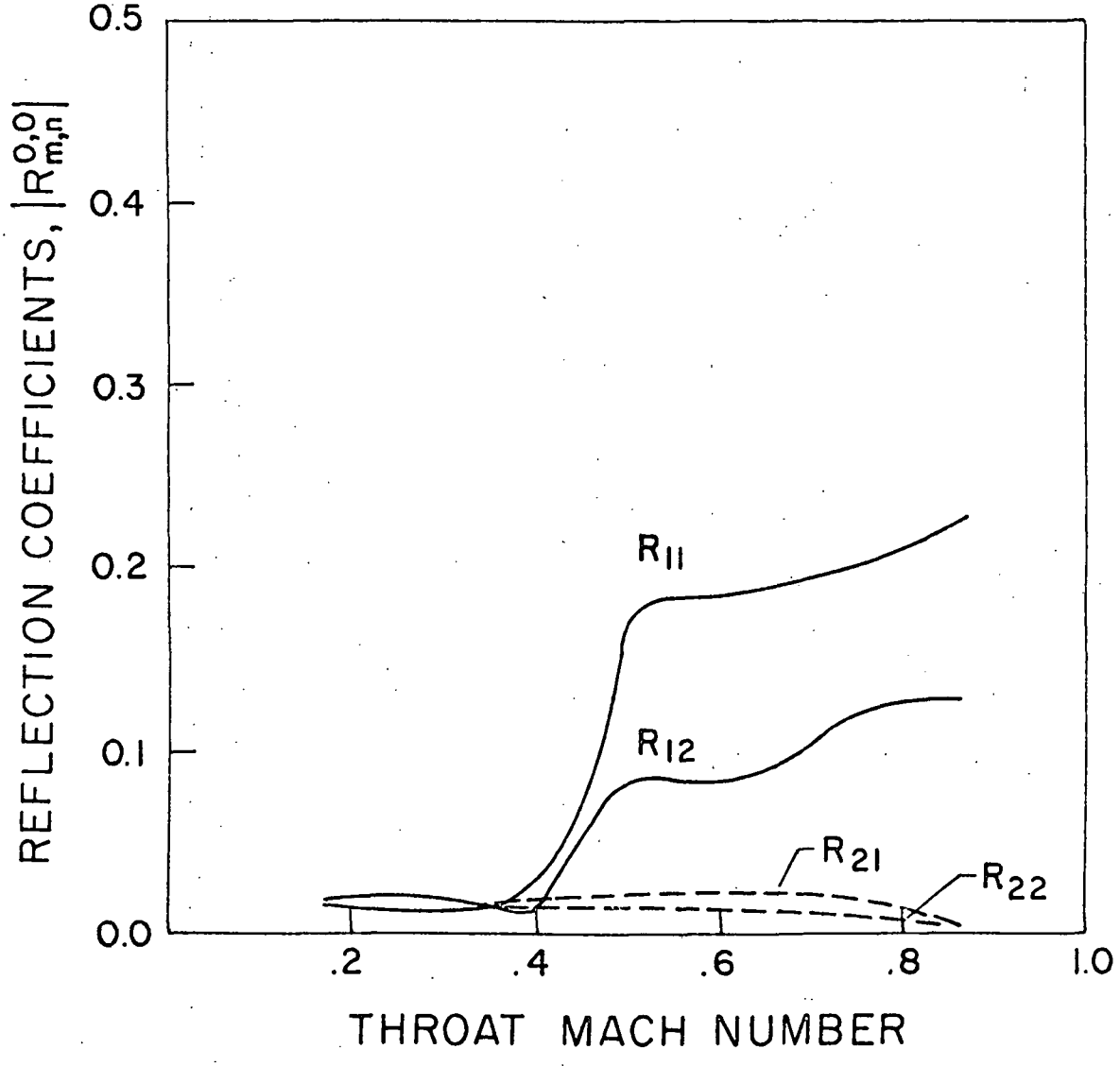

Figure 15. Effect of the throat Mach number on the absolute value of the reflection coefficients in a lined duct; right-running modes incident at $x = 0$; $\omega = 7$, $N = 2$.

6. CONCLUSIONS AND RECOMMENDATIONS

An acoustic theory is developed to determine the sound transmission and attenuation through an infinite, hard-walled or lined circular duct carrying compressible, sheared, mean flows and having a variable cross section. The theory is applicable to large as well as small axial variations, as long as the mean flow does not separate. The technique is based on solving for the envelopes of the quasi-parallel acoustic modes that exist in the duct instead of solving for the actual wave, thereby reducing the computation time and the round-off error encountered in purely numerical techniques. The solution recovers the solution based on the method of multiple scales for slowly varying duct geometry.

A computer program has been developed based on this theory for general mean flows. Numerical calculations performed for waves propagating in uniform ducts carrying fully developed mean flows agree with the well-known results for uniform ducts. To investigate the effect of the axial variations of the flow and the duct geometry, calculations using a simple mean-flow model have been performed. The model consists of a one-dimensional flow in an inviscid core and a quarter-sine profile in the boundary layer.

Results are presented for the reflection and transmission coefficients in ducts with varying slopes and carrying different mean flows. The main conclusions are:

1. Axial variations of the duct properties and the mean flow produce coupling between the modes.

2. It is found that coupling between modes travelling in opposite directions can be significant for some cases with a mean flow in contrast with the no-mean-flow case.

3. At high Mach numbers the wavenumbers for the upstream modes become very large, and the nonlinear terms must be included.

4. Overall direct transmission coefficients decrease when the duct wall is lined, but the addition of a liner may lead to an increase in the intermodal transmission coefficients in some cases.

5. As the throat Mach number increases, the transmission coefficients are reduced; however, the coefficients for the upstream modes are reduced more than those of the downstream modes.

6. The addition of a liner may lead to an increase in the reflection coefficients.

The only limitation of the wave envelope technique is that it is not suitable near cut off, since the coefficient multiplying the term $\frac{dA_n}{dx}$ approaches zero. This problem is more apparent for a hard wall duct than for a soft wall duct, because k is exactly zero for a hard wall duct. Near cut off, the problem requires a turning-point analysis using either the method of multiple scales or the Langer transformation[33].

Although the present theory is an important step towards qualitatively understanding the physical mechanisms responsible for noise reduction in choked or partially-choked inlets, it cannot be applied to actual inlet configurations. To accomplish this, one needs to extend the present work by (1) coupling the present program with a computer code that calculates the actual mean flow in such inlets, (2) including the nonlinear terms in the acoustic equations, and (3) incorporating a turning-point analysis for cases when modes approach cut-off conditions.

REFERENCES

1. Maestrello, L., "The Design and Evaluation of an Aerodynamic Inlet Noise Suppressor," Boeing Document D6-5980, 1960.
2. Lumsdaine E., "Development of a Sonic Inlet for Jet Aircraft," Internoise '72 Proceedings, pp. 501-506, 1972.
3. Klujber, F., Bosch, K. C., Demetrick, S. R. and Robb, W. R., "Investigation of Noise Suppression by Sonic Inlets for Turbofan Engines," Boeing Document D6-40855, NASA CR-121126, CR-121127, July, 1973.
4. Sobel, J. A. and Welliver, A. D., "Sonic Block Silencing for Axial and Screw-Type Compressors," Noise Control, Vol. 7, No. 5, pp. 9-11, Sept/Oct., 1961.
5. Greatrex, F. B., "By-Pass Engine Noise," Trans. SAE, Vol. 69, pp. 312-324, 1961.
6. Sawhill, R. H., "Investigation of Inlet Airflow Choking as a Mean of Suppressing Compressor Noise - 5' Inlet Model," Boeing Documents D6A-10155-1, 1966.
7. Cawthorne, J. M., Morris, G. J., and Hayes, C., "Measurement of Performance, Inlet Flow Characteristics, and Radiated Noise for a Turbojet Engine Having Choked Inlet Flow," NASA TN D-3929, 1967.
8. Anderson, A. O., "An Acoustic Evaluation on the Effect of Choking using a Modal Supersonic Inlet," Boeing Document D6A-10378-1, 1966.
9. Schaut, L. A., "Results of an Experimental Investigation of Total Pressure Performance and Noise Reduction of an Airfoil Grid Inlet," Boeing Document D6-23276, 1969.

10. Anderson, R., Destafanis, P., Farguhar, B. W., Giarda, G., Shuehle, A., and Van Duine, A. A., "Boeing/Aeritalia Sonic Inlet Feasibility Study," Boeing Document D6-40208, 1972.

11. Chestnutt, D. and Stewart, N. D., "Axial Flow Compressor Noise Reduction by Means of Inlet Guide Van Choking," NASA Langley Working Paper, LWP-473, Nov. 1967.

12. Chestnutt, D., "Noise Reduction by Means of Inlet-Guide-Vane Choking in an Axial-Flow Compressor," NASA TN D-4682, 1968.

13. Copeland, W. L., "Inlet Noise Suppression Test," Boeing Document T6-3173, 1974.

14. Hawking, D. L. and Lawson, M.V., "Theoritical Investigation of Supersonic Rotor Noise," Loughborough University Report TT7213, Dec. 1972.

15. Benzakein, M. J., Kazin, S. B. and Savell, C. T., "Multiple Pure-Tone Noise Generation and Control," AIAA Paper No. 73-1021, October 1973.

16. Klujber, F., "Results of an Experimental Program for the Development of Sonic Inlets for Turbofan Engines," AIAA Paper No. 73-222.

17. Higgins, C. C., Smith, J. N., and Wise, W. H., "Sonic Throat Inlets," NASA SP-189, pp. 197-215, 1968.

18. Lumsdaine, E., Cherng, J. G., Tag, I., and Clark, L. R., "Noise Suppression with High Mach Number Inlets," NASA-CR-143314, July, 1975.

19. Koch, R. L., Ciskowski, T. M., and Garzon, J. R., "Turbofan Noise Reduction Using a Near Sonic Inlet," AIAA Paper No. 74-1098, 1974.

20. Miller, B. A. and Abbott, J. M., "Aerodynamic and Acoustic Performance of Two Choked Flow Inlets under Static Conditions," NASA-TM-X-2629-E7008.

21. Abbott, J. M., "Aeroacoustic Performance of Scale Model Sonic Inlets - Takeoff/Air Approach Noise Reduction," AIAA Paper No. 75-202, 1975.

22. Groth, H. W., "Sonic Inlet Noise Attenuation and Performance with a J-85 Turbojet Engine as a Noise Source," AIAA Paper No. 74-91, 1974.

23. Savkar, S. D. and Kazin, S. B., "Some Aspects of Fan Noise Suppression Using High Mach Number Inlets," AIAA Paper No. 74-554, 1974.

24. Miller, B. A., "Experimentally Determined Aeroacoustic Performance and Control of Several Sonic Inlets," AIAA Paper No. 75-1184, 1975.

25. Chestnutt, D. and Clark, L. R., "Noise Reduction by Means of Variable-Geometry Inlet Guide Vanes in a Cascade Apparatus," NASA TN X-2392, 1971.

26. Nayfeh, A. H., Kaiser, J. E., and Telionis, D. P., "Acoustics of Aircraft Engine-Duct Systems," AIAA Journal, Vol. 13, pp. 130-153, 1975.

27. Nayfeh, A. H., "Sound Propagation Through Nonuniform Ducts," Proceedings of the Society of Engineering Science at NASA Langley Research Center, November 1-3, 1976.

28. Webster, A. G., "Acoustical Impedance and the Theory of Horns and of the Phonograph," Proceedings of the National Academy of Science, Vol. 5, pp. 275-282, 1919.

29. Stevenson, A. F., "Exact and Approximate Equations for Wave Propagation in Acoustic Horns," Journal of Applied Physics, Vol. 22, pp. 1461-1463, 1951.

30. Eversman, W., Cook, E. L., and Beckemeyer, R. J., "A Method of Weighted Residuals for the Investigation of Sound Transmission in Non-Uniform Ducts without Flow," Journal of Sound and Vibration, Vol. 38, pp. 105-123, 1975.

31. Alfredson, R. J., "The Propagation of Sound in a Circular Duct of Continuously Varying Cross-Sectional Area," Journal of Sound and Vibration, Vol. 23, 1972.

32. Nayfeh, A. H. and Telionis, D. P., "Acoustic Propagation in Ducts with Varying Cross-Sections," Journal of the Acoustical Society of America, Vol. 54, No. 6, pp. 1654-1661, 1973.

33. Nayfeh, A. H., Perturbation Methods, Wiley-Interscience, New York, Chapter 6, 1973.

34. Isakovitch, M. A., "Scattering of Sound Waves on Small Irregularities in a Wave Guide," Akusticheskii Zhurnal, Vol. 3, 1957.

35. Samuels, J. S., "On Propagation of Waves in Slightly Rough Ducts," The Journal of the Acoustical Society of America, Vol. 31, March 1959, pp. 319-325.

36. Salant, R. F., "Acoustic Propagation in Waveguides with Sinusoidal Walls," The Journal of the Acoustical Society of America, Vol. 53, Feb. 1973, pp. 504-507.

37. Nayfeh, A. H., "Acoustic Waves in Ducts with Sinusoidally Perturbed Walls and Mean Flow," Journal of the Acoustical Society of America, Vol. 57, pp. 1036-1039, 1975.

38. Quinn, D. W., "A Finite Difference Method for Computing Sound Propagation in Nonuniform Ducts," AIAA Paper NO. 75-130, 1975.

39. Baumeister, K. J. and Rice, E. J., "A Difference Theory for Noise Propagation in an Acoustically Lined Duct with Mean Flow," AIAA Paper 73-1007, 1973.

40. Baumeister, K. J., "Generalized Wave Envelope Analysis of Sound Propagation in Ducts with Variable Axial Impedance and Stepped Noise Source Profiles," AIAA Paper No. 75-518, 1975.

41. Powell, A., "Theory of Sound Propagation through Ducts Carrying High-Speed Flows," Journal of the Acoustical Society of America, Vol. 32, pp. 1640-1946, 1960.

42. Eisenberg, N. A. and Kao, T. W., "Propagation of Sound Through a Variable-Area Duct with a Steady Compressible Flow," Journal of the Acoustical Society of America, Vol. 49, pp. 169-175, 1971.

43. Davis, S. S. and Johnson, M. L., "Propagation of Plane Waves in a Variable Area Duct Carrying a Compressible Subsonic Flow," presented at the 87th Meeting of the Acoustical Society of America, New York, 1974.

44. Huerre, P. and Karamcheti, K., "Propagation ofound through a Fluid Moving in a Duct of Varying Area," in Interagency Symposium of University esearch in Transportation Noise, Stanford, Vol. II, pp. 397-413, 1973.

45. King, L. S. and Karamcheti, L., "Propagation of Plane Waves in the Flow Through a Variable Area Duct," AIAA Paper 73-1009, 1973.

46. Nayfeh, A. H., Telionis, D. P., and Lekoudis, S. G., "Acoustic Propagation in Ducts with Varying Cross Sections and Sheared Mean Flow," AIAA Paper No. 73-1008, 1973.

47. Nayfeh, A. H., Kaiser, J. E., and Telionis, D. P., "Transmission of Sound Through Annular Ducts of Varying Cross Sections," AIAA Journal, Vol. 13, No. 1, pp. 60-65, 1975.

48. Nayfeh, A. H., Kaiser, J. E., "Effect of Compressible Sheared Mean Flow on Sound Transmission Through Variable-Area Plane Ducts," AIAA Paper 75-128, 1975.

49. Eversman, W., "A Multimodal Solution for the Transmission of Sound in Nonuniform Hard Wall Ducts with High Subsonic Flow," AIAA Paper No. 76-497, 1976.

50. Kaiser, J. and Nayfeh, A. H., "A Wave-Envelope Technique for Wave Propagation in Nonuniform Ducts," AIAA Journal, Vol. 15, No. 4, pp. 533-537, April 1977.

51. Schlicting, H., Boundary-Layer Theory, 6th Ed., McGraw-Hill, New York, pp. 61-254, 1968.

52. Nayfeh, A. H., "Effect of the Acoustic Boundary Layer on the Wave Propagation in Ducts," Journal of the Acoustical Society of America, Vol. 54, No. 6, pp. 1737-1742, Dec. 1973.

53. Pestorius, F. M., and Blackstock, D. T., "Nonlinear Distortion in the Propagation of Intense Acoustic Noise," Interagency Symposium on University Research in Transportation Noise Proceedings, Vol. II, pp. 565-577, 1973.

54. Nayfeh, A. H. and Sun, J., "Effect of Transverse Velocity and Temperature Gradients on Sound Attenuation in Rectangular Ducts," Journal of Sound and Vibration, Vol. 34, No. 4, pp. 505-517, June, 1974.

55. Zorumski, W. E., "Acoustic Theory of Axisymmetric Multisectioned Ducts", NASA TR R-419, May 1974.